University of Helsinki
Faculty of Science
Department of Chemistry
Laboratory of Radiochemistry
Finland

ORIGIN DETERMINATION OF REACTOR PRODUCED PLUTONIUM BY MASS SPECTROMETRIC TECHNIQUES: APPLICATION TO NUCLEAR FORENSIC SCIENCE AND SAFEGUARDS

Maria Wallenius

Academic Dissertation
To be presented with the permission of the Faculty of Science of the University of Helsinki for public criticism in the small lecture hall A129 of the Department of Chemistry on 17th February, 2001, at 12 o'clock noon.

Helsinki 2001

ISBN 951-45-9707-9 (nid.)
ISBN 951-45-9708-7 (PDF)
ISSN 0358-7746
Helsinki 2001
Yliopistopaino

PREFACE

The present study was carried out in the Institute for Transuranium Elements (ITU) in the Nuclear Chemistry unit, European Commission, Joint Research Centre, Karlsruhe, Germany, during 1996-2000 with a grant from the European Commission.

I would like to express my acknowledgement to several people, who have made this thesis possible.

Prof. Timo Jaakkola, who directed me towards the world of mass spectrometry between 1994 and 1996, when I was working in the Laboratory of Radiochemistry in the University of Helsinki. Later your support and encouragement during the thesis were highly appreciated.

Dr. Lothar Koch, who guided me into the interesting area of nuclear forensic science. Your enormous knowledge and experience impressed me deeply. I thank you for the valuable discussions, which helped me in all stages of the thesis. It was an honour to work with you.

Dr. Roland Schenkel, the director of the ITU and Dr. Jacques van Geel, the former director of the ITU.

Dr. Klaus Mayer, who deepened my knowledge in the mass spectrometry by his valuable advices.

Dr. Maria Betti, who made it possible for me to have a grant and do my thesis in the ITU.

Dr. Gabriele Tamborini, who helped me in the field of SIMS.

Dr. Paolo Peerani, who helped me to understand the basics of reactor physics.

Mr. Fabio Bocci, who performed the ICP-MS measurements.

Dr. Joseph Magill, who revised the language of the thesis.

I wish also to thank all my colleagues of the Nuclear Chemistry group for their help.

Finally, my deepest thanks to my parents for all the support and to Louis-Olivier Actis-Dato for standing by my side and giving the love and happiness.

ABSTRACT

The age and production type, i.e. origin, are highly important parameters to be revealed when seized Pu from illicit trafficking has to be analysed. In addition, in a view of pending Fissile Material Cut-off Treaty, the age determination of Pu enables to control the agreement.

The ages of Pu bulk samples were determined from the $^{238}Pu/^{234}U$, $^{239}Pu/^{235}U$ and $^{240}Pu/^{236}U$ ratios by IDMS and the results were compared to the ages obtained from the $^{241}Pu/^{241}Am$ ratio by gamma-spectrometry. The ages from three different Pu/U ratios were uniform showing that the Pu/U separation, when reprocessing the spent fuel, was complete. Small differences between ages from the Pu/U and Pu/Am ratios were observed, giving consistently higher ages of a few per cent from the $^{241}Pu/^{241}Am$ ratio. This is most likely due to the Am traces remained in Pu after the reprocessing.

Particle analyses were performed from the above mentioned Pu/U ratios by SIMS. Due to the different ionisation efficiencies of Pu and U, a relative sensitivity factor (RSF) had to be determined for the Pu/U ratio. The RSF was then applied to correct the measured ratios. The SIMS showed its strength when using the technique to determine the age of powder mixtures. The ages of different components are possible to reveal, which is a big advantage compared to the bulk analysis, where this is not possible.

The production of the Pu material, i.e. the reactor type, was determined using the isotopic correlation technique. The Pu compositions for different spent fuels (Candu, LWR, graphite-moderated LWR, Magnox, fast reactor and typical research reactors) were calculated by ORIGEN2 and SCALE computer codes and they were plotted in the graph, which separates the reactor types depending on their characteristic neutron spectra and initial ^{235}U enrichments. The reactor types were possible to reveal in most of the cases and when not, these reactor types could be excluded to be the origin.

A new detector type TIMS, Multi-Micro-Channeltron-TIMS, was introduced. The MMC-TIMS allows the reduction of the needed sample amount by a factor of 1000 compared to the conventional Faraday cup detector TIMS. This is very important because it is desired to manage as small samples as feasible when handling health hazardous materials like actinides.

LIST OF PUBLICATIONS

This dissertation is based on the following publications:

I **Age determination of plutonium material in nuclear forensics by thermal ionisation mass spectrometry**

M. Wallenius, K. Mayer, Fresenius' Journal of Analytical Chemistry Vol. 366, No.3, 2000, 234-238

II **The "age" of plutonium particles**

M. Wallenius, G. Tamborini, L. Koch, Radiochimica Acta, in press

III **Origin determination of plutonium material in nuclear forensics**

M. Wallenius, P. Peerani, L. Koch, Journal of Radioanalytical and Nuclear Chemistry, Vol. 246, No. 2, 2000, 317-321

IV **First performance tests of a Multi-Micro-Channeltron thermal ionisation mass spectrometer**

M. Wallenius, H. Kühn, K. Mayer, L. Koch, Advances in Mass Spectrometry, Vol. 14, CD-ROM version, 1998

These publications are referred to in the text by their Roman numerals. The summary contains also some more recent results which are not mentioned in the publications.

TABLE OF CONTENTS

1. Introduction

At the end of 1998, there was over 1350 tons of plutonium (Pu) in the world. This Pu has been produced either as a by-product from spent nuclear fuels (~1100 t) or for nuclear weapons (~250 t) [1]. Pu has been produced mainly by a few countries, i.e. nuclear weapon countries and countries which produce a lot of their energy by nuclear power. These countries include USA, Canada, Russia, France, United Kingdom, Germany and Japan.

The diversion of Pu is a big issue, not only because of its hazardous nature, but also in a view of non-proliferation. Most of the Pu is in spent fuel form, i.e. it has not been separated from the uranium and fission products. This Pu is hardly a matter of concern in a view of proliferation of the nuclear weapon material, because it is very dangerous and thus difficult to transport due to its high radioactivity of fission products. This makes it also easy to detect. Separated Pu for nuclear weapons or for the use of MOX fuel is, in the other hand, much easier to transport, because of its relatively low radioactivity and small size (i.e. a size of soft-drink can is ~7 kg of Pu).

In the beginning of 1990's, the break-up of the Soviet Union caused a problem for the safeguarding of the nuclear material. The Former Soviet Union countries (e.g. Ukraine, Belarus, Kazakhstan and Lithuania) had suddenly large amounts of Pu and high enriched uranium (HEU) and, at the same time, no proper legislation or control of the material was available. As a consequence of this, some nuclear material was lost and first illicit trafficking incidents of nuclear material occurred. In the year 1994, a total of 42 smuggling cases of nuclear material were detected. This was 65 % of the total smuggling incidents, which includes also radioactive sources. Since then the number of cases has decreased year by year and in the 1999 (till end of August) only 4 smuggling incidents of nuclear material were recorded in the IAEA's illicit trafficking database [2].

The concern about the growth of nuclear weapon material brought about the discussion on cut-off the fissile material production for nuclear weapons at the initiative of the President Clinton in 1993. The Fissile Material Cut-off Treaty (FMCT) would ban the Pu and HEU production for use of nuclear weapons and other nuclear explosive devices. The treaty would cover all the sensitive fissile material production facilities, i.e. enrichment, reprocessing and fabrication plants.

Nuclear forensic science is a new multidisciplinary area, which deals with the identification and determination of nuclear materials mostly in a context of criminal investigation. It uses the characteristics inherent to a nuclear material to obtain information on the origin and production

route of the sample under investigation. The first nuclear forensic case could be said to be the “Oklo” - a uranium mine situated in Gabon, Africa. In 1972 it was noticed that the enrichment of the natural U was lower in Oklo than normally. By studying the fission products found, it was observed that there had been a natural nuclear reactor operating about 1.8 billion years ago [3,4]. Even if the nuclear forensics implies typically the analyses of uranium and plutonium material, sometimes analyses of non-nuclear elements are also performed. This is specially the case, when scrap material is sold in black-markets as nuclear weapon usable material. The most notorious nuclear hoax is so-called “Red Mercury” [5,6].

In this study a methodology to determine the origin of reactor produced Pu was developed, which can be used in the case of seized Pu and for the cut-off treaty. The origin means in this context the age, i.e. the time that has passed since the Pu material was reprocessed or purified, and production type, i.e. the reactor type where the Pu was produced. These two parameters, together with the impurity and microstructure analyses and databank, make it possible, though not in every case, to find the exact origin. At least these data can be used to exclude the place where the material cannot originate. To determine these parameters accurately and precisely, which is the necessity due to the sensitive nature of the subject, mass spectrometric techniques, TIMS, SIMS and ICP-MS, were chosen. These techniques are known to represent state of the art in isotope ratio and content determination for the varying sample sizes contained in this study.

2. Nuclear forensic science

Forensic science is comprised of several technical disciplines that are applied to matters of law. For example, forensic toxicology concerns the examination of body fluids, tissues, and other biological material in order to detect poisons that may relate to the cause and manner of death. Forensic geology deals with soils including minerals, fossils, trace metals, and dissolved rocks, where the soil composition reflects glacial movements and climatic conditions. Forensic chemistry is principally an application of analytical chemistry within a legal context, and it includes arson chemistry, explosives, drugs and trace evidences (e.g. in glass, paints). During the last decade, nuclear material has become a part of the forensic sciences and a new branch - nuclear forensics - has developed.

In nuclear forensics, unknown uranium or plutonium containing material has to be analysed and its origin, intended use and production route unravelled. This can be done using the characteristics inherent to the nuclear material. The possible sources of nuclear forensic samples are: 1) operational and accidental releases from nuclear installations, 2) atmospheric and underground bomb tests, and 3) diversion from weapon production or commercial fuel cycle, i.e. illicit trafficking. There is no fixed scheme of analysis for unknown nuclear material, which is contrary to the present verification analysis for a declared nuclear material, but it is guided by the pattern of information that builds up during the investigation. Nuclear material analysis, though essential, is only a part of nuclear forensics. Therefore information of intelligence services as well as the circumstance of seizing or sampling the material has to also be considered.

2.1 Illicit trafficking

Illicit trafficking involves unauthorised movement of nuclear material and other radioactive sources. Illicit trafficking of nuclear material has arisen in the beginning of the 1990's, which has been believed mainly to be due to the disruption of the Former Soviet Union (FSU). Undeveloped inventory control and security together with 75 tons stockpile of plutonium and several hundred tons of highly enriched uranium (≥20 % ^{235}U) from disarmament of Cold War nuclear weapons scattered among 80 to 100 facilities enabled easier diversion of nuclear material. Besides this, it has been estimated that Russia has between 35 and 50 tons of plutonium in the form of solutions, scrap and residues [7]. Total military plutonium amount in the world is about 250 tons, and over

90 % of that is in separated form. Additionally, at the end of 1998, 200 tons of separated plutonium from civil nuclear power plants have been estimated existing [1].

Since the beginning of 1993, over 300 smuggling incidents of nuclear material and radioactive sources have been listed in the IAEA illicit trafficking database. 265 of the cases have been confirmed by Member States [2]. Main part of the seizures and also the most serious ones were made in Germany, the Czech Republic and Russia (Fig.1). In 1993-1996 over 60 % of the smuggling incidents were nuclear material. The rest were radioactive sources, like ^{137}Cs- or ^{60}Co-sources used in the medicine and research. Since then the number of nuclear material cases has decreased and in 1999 their proportion was only 20 %. The smuggled nuclear material has contained mainly depleted, natural or low enriched uranium for use in nuclear power reactors, but a number involving weapon-utilisable nuclear material, i.e. highly enriched uranium (HEU) or plutonium, have also occurred (Table 1) [8,9].

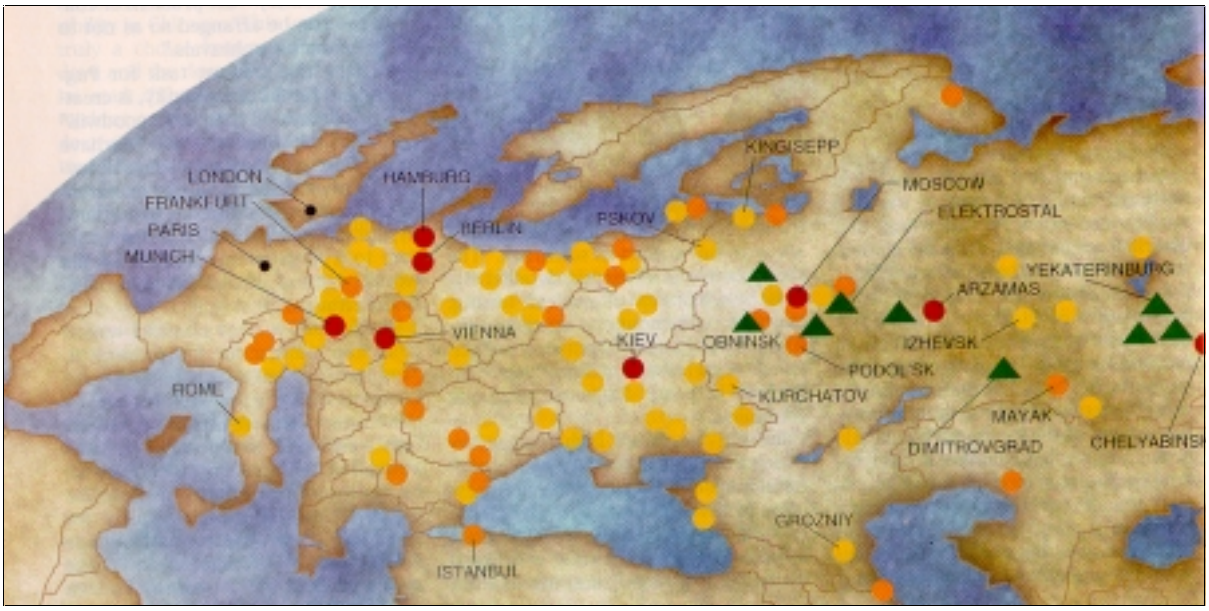

Fig.1. Sites of nuclear smuggling incidents in Europe and FSU by 1995 [8].

- 5 or more
- 2 to 4
- 1
- ▲ Nuclear stockpiles, reprocessing plants or weapons-design laboratories

The quantities of the smuggled plutonium and HEU have been, until now, too low to make a nuclear weapon as it is known that a nuclear bomb requires between three and 25 kilograms of HEU or between one and eight kilograms of plutonium depending on the composition and the production technology [8]. However, trafficking of small quantities of such material can help to accumulate larger quantities of nuclear material of strategic value in the context of non-

proliferation. Potential customers of the smuggled nuclear material have been considered to be terrorist groups and on the other hand, in the light of proliferation, rogue nations like Iraq, Iran and Libya [10].

Table 1. Smuggled plutonium and HEU incidents [2].

Date	Place	Quantity and type of material
10.05.1994	Tengen, Germany	5.6 g ^{239}Pu (0.18 % ^{240}Pu)
25.07.1994	Munich, Germany	240 mg ^{239}Pu (11.4 % ^{240}Pu) and 170 mg HEU (36.5 %)
10.08.1994	Munich airport, Germany	363 g ^{239}Pu (10.78 % ^{240}Pu) and 560 g LEU
12.08.1994	Bremen, Germany	0.05 mg Pu
03.1994	Electrostal, Russia	2.972 kg HEU (90 %)
13.06.1994	Landshut, Germany	0.8 g HEU (87.8 %)
14.12.1994	Prague, Czech Republic	2.73 kg HEU (87.7 %)
06.1995	Electrostal, Russia	1.7 kg HEU (20 %)
06.06.1995	Prague, Czech Republic	0.415 g HEU (87.7 %)
08.06.1995	Ceske Budejovice, Czech Republic	16.958 g HEU (87.7 %)
29.05.1999	Rousse, Bulgaria	10 g HEU (>20 %)

2.1.1 Programmes to prevent illicit trafficking

After the explosive increase of illicit trafficking incidents in the beginning of 1990's, actions to prevent further incidents of illicit trafficking were worked out. In 1994 IAEA launched a programme, Security of Material, to address illicit trafficking of nuclear material and other radioactive sources. The programme has been arranged between IAEA and its Member States with close co-operation of scientific community, law enforcement organisations and transporters, such as United Nations, the European Union, Interpol, Europol, Euratom, International Air Transport Association, International Road Transport Union, World Custom Organisation and the Universal Postal Union. The programme has focused on four main activities: prevention, response, training and the exchange of information. Firstly in greater detail, the prevention part of the programme helps countries to strengthen their basic nuclear laws and infrastructures, to upgrade their accounting, control and security of nuclear and radioactive sources, as well as improve their control of the import and export of strategic goods and materials. Secondly, the response part

helps countries to detect and react to illegal cross-border movements of radioactive materials and analyse confiscated material. Additionally it provides authoritative and timely information on trafficking incidents reported to the IAEA illicit trafficking database, in which currently 60 States* are participating. Thirdly, the programme develops and provides training opportunities for both state regulatory and facility personnel, and fourthly, it enhances the exchange of information via international and inter-agency meetings and conferences [12,13].

The United States of America have developed programmes for a co-operation with Russia to strengthen the security of the nuclear warheads and nuclear materials. In 1991 the congress launched the "government-to-government" programme called Nunn-Lugar to assist the former Soviet Union in the transportation, storage, safeguarding, destruction of nuclear weapons and the prevention of weapon proliferation. Additionally, the DOE started a so called "lab-to-lab" programme, in which materials security experts at its national laboratories were authorised to approach their Russian counterparts directly to propose joint work on material security [14].

* Argentina, Australia, Austria, Bangladesh, Belarus, Belgium, Bolivia, Brazil, Bulgaria, Canada, Chile, Croatia, Cuba, Cyprus, the Czech Republic, Denmark, the Dominican Republic, Ecuador, Estonia, Finland, France, Georgia, Germany, Ghana, Greece, Hungary, Israel, Italy, Japan, Latvia, Lithuania, Mexico, Morocco, Namibia, the Netherlands, New Zealand, Nigeria, Norway, Peru, the Philippines, Poland, Portugal, the Republic of Korea, Romania, the Russian Federation, Saudi Arabia, the Slovak Republic, Slovenia, South Africa, Spain, Sri Lanka, Sweden, Switzerland, Tunisia, Turkey, Ukraine, United Kingdom, the United States of America, Venezuela and Vietnam [11]

2.1.2 International Technical Working Group on Nuclear Smuggling

To recognise the capability of nuclear forensics, the P-8 countries encouraged technical experts to evaluate the role of nuclear forensics in combating nuclear smuggling and possibly developing mechanisms for international co-operation. As a result, an International Conference on Nuclear Smuggling Forensic Analysis was held in November 1995 at the Lawrence Livermore National Laboratory, USA. The International Conference comprised scientists, law enforcement and intelligence experts from 14 countries and organisations and it culminated with plans to found a Nuclear Smuggling International Technical Working Group (ITWG). The first meeting of ITWG was held in January 1996 at the Institute for Transuranium Elements in Karlsruhe, Germany and since then it has had meetings yearly [15,16]. One of its first tasks was to make an inventory of the technical tools available at that time for nuclear forensic analyses. It was soon recognised that new methods had to be developed to meet novel requirements. Later, in 1998 ITWG initiated its first inter-laboratory exercise, called Round-Robin test, on Pu to evaluate and improve the

effectiveness of forensic techniques and methods [17]. The second Round-robin test on HEU is planned to be organised in 2001 [18].

2.2 Endogenous information

Material that underwent nuclear processes shows an inherent consistency of its nuclides, which point back to the nuclear processes in which the material was involved. Thus such so-called endogenous information is self-explanatory and requires no verification by comparison with material of established history. From this endogenous information, the general origin (i.e. the age and production mode) and the intended use of the material can be determined.

When considering reactor produced Pu material, a lot of information has been lost when the spent fuel has been reprocessed. Thus the useful information of the fission products and minor actinides are mostly gone and the origin of Pu material can be found out only from the information obtained from Pu isotopes themselves and their in-growing daughter nuclides.

2.2.1 Age

Age determination or dating is very commonly used in geo- and cosmochemistry. Several parent/daughter relations exist, from which the age can be determined. Most commonly used dating methods for rocks and minerals are: ^{40}K-^{40}Ar, ^{40}K-^{40}Ca, ^{87}Rb-^{87}Sr, ^{147}Sm-^{143}Nd, ^{176}Lu-^{176}Hf, ^{187}Re-^{187}Os, ^{235,238}U,^{232}Th-^{206,207,208}Pb [19].

Age determination is based on the decay of a radioactive parent nuclide N to its daughter nuclide D. The rate of decay of a radioactive nuclide is expressed:

$$-\frac{dN}{dt} = \lambda N \qquad (1)$$

where λ is the decay constant ($\ln 2 / T_{1/2}$) of the nuclide. From the equation 1, the basic equation describing all radioactive decay processes is formed:

$$N = N_0 e^{-\lambda t} \qquad (2)$$

where N is the number of remained atoms of the parent nuclide after time t and N_0 is the number of atoms of the parent nuclide in the beginning. The number of stable daughter atoms (D) produced by the decay is given by:

$$D = N_0 - N \quad (3)$$

$$D = N_0 - N_0 e^{-\lambda t} \quad (4)$$

$$D = N_0 (1 - e^{-\lambda t}) \quad (5)$$

Equation 5 is valid for all above-mentioned dating methods, where the decay product is stable. However, this is not valid for Pu, whose daughter nuclides are all radioactive and decaying further. In this case the decay rate of the daughter nuclide N_2 is the difference between the rate at which it is produced by decay of N_1 (parent nuclide) and its own decay rate:

$$\frac{dN_2}{dt} = \lambda_1 N_1 - \lambda_2 N_2 \quad (6)$$

The number of formed daughter nuclides after time t is expressed by the equation:

$$N_2 = \frac{\lambda_1}{\lambda_2 - \lambda_1} N_1^0 (e^{-\lambda_1 t} - e^{-\lambda_2 t}) + N_2^0 e^{-\lambda_2 t} \quad (7)$$

If the initial number of daughter atoms N_2^0 is zero, the equation 7 reduces to:

$$N_2 = \frac{\lambda_1}{\lambda_2 - \lambda_1} N_1^0 (e^{-\lambda_1 t} - e^{-\lambda_2 t}) \quad (8)$$

The “age” of the Pu expresses the time that has passed since the Pu was last time chemically processed, i.e. reprocessed or purified. The age can be determined for reactor produced Pu from a few parent/daughter ratios, which are: $^{238}Pu/^{234}U$, $^{239}Pu/^{235}U$, $^{240}Pu/^{236}U$, $^{241}Pu/^{241}Am$ and $^{242}Pu/^{238}U$ (equations 9-13).

$$\mathbf{^{238}Pu} \xrightarrow[\alpha]{87.76\ a} \mathbf{^{234}U} \longrightarrow \ldots\ldots \longrightarrow {}^{206}Pb\ (stable) \quad (9)$$

$$^{239}\mathbf{Pu} \xrightarrow[\alpha]{24130\ a} {}^{235}\mathbf{U} \longrightarrow \ldots\ldots \longrightarrow {}^{207}\mathrm{Pb\ (stable)} \quad (10)$$

$$^{240}\mathbf{Pu} \xrightarrow[\alpha]{6568\ a} {}^{236}\mathbf{U} \longrightarrow \ldots\ldots \longrightarrow {}^{208}\mathrm{Pb\ (stable)} \quad (11)$$

$$^{241}\mathbf{Pu} \xrightarrow[\beta^-]{14.41\ a} {}^{241}\mathbf{Am} \longrightarrow \ldots\ldots \longrightarrow {}^{209}\mathrm{Bi\ (stable)} \quad (12)$$

$$^{242}\mathbf{Pu} \xrightarrow[\alpha]{373800\ a} {}^{238}\mathbf{U} \longrightarrow \ldots\ldots \longrightarrow {}^{206}\mathrm{Pb\ (stable)} \quad (13)$$

Later in the dating, some assumptions have been made concerning the parent/daughter-system:

1) No daughter nuclide was present at the start of decay time, i.e. the parent was completely separated from the daughters at one point of time.
2) The system was not altered during the time under consideration, i.e. the daughter was not separated, partially or wholly from the parent, and neither parent nor daughter was added to the system at any time.

2.2.2 Production type

The production type, i.e. the reactor type, of plutonium can be deduced from the isotopic abundances that are unchanged by chemical processes. Plutonium composition varies significantly between different reactor types depending on the neutron energy spectrum and the initial ^{235}U enrichment of the reactor. For example, with increasing ^{235}U enrichment, the build-up of ^{238}Pu is enhanced, whereas the hardening of the neutron spectrum leads to lower abundances of the higher Pu isotopes. Additionally the neutron flux affects the production of Pu isotopes causing relatively higher amounts of the ^{240}Pu compared to the ^{239}Pu at higher fluxes.

After the reactor type is determined, the result helps to identify the reprocessing plant. One reprocessing plant usually reprocess only one type of reactor fuel, thus finding out the reactor type (i.e. HWR, LWR, RBMK, FBR, and research reactor), the origin can be limited to such reprocessing plants which reprocess the spent fuel in question. Since it is in most cases known where the reprocessing plants obtain their spent fuels, the origin can be confined to these reactors.

2.2.3 Intended use

The isotopic composition of uranium and plutonium points directly to the intended use of nuclear material. There are three categories into which nuclear material can fall (Table 2).

Table 2. Nuclear material classification [15].

Nuclide	Concentration	Classification
^{239}Pu ^{235}U	> 90 % > 93 %	weapons grade
^{239}Pu, ^{241}Pu ^{235}U	any concentration > 20 %	weapons-utilisable
^{235}U	< 20 %	non-weapons utilisable

Intended use can be recognised also by the chemical composition of metallic or ceramic material, or by the dimensions of fuel pellets. This, however, concerns more uranium and, on the other hand, a databank including these particular parameters is required to interpret this kind of information (Chapter 2.3.).

2.3 Exogenous information

From the fabrication of a nuclear material, traces of non-nuclear elements remain and they are characteristic of the production technology, reagent composition and geographic location where the material was produced. To link the results of an investigation to a particular process and/or production facility, the corresponding process parameters have to be known. To some extent they can be found in the open literature, but the specified data such as material structure and impurities are often known only in the respective facility. Therefore a databank, which contains such exogenous information, is required to interpret the data. Since 1996, data from the fuel manufacturers have been collected in identical databanks established in the Institute of Transuranium Elements, Karlsruhe, Germany and Bochvar's Research Institute of Inorganic Materials, Moscow, Russia [20-22]. The databanks include data on fresh nuclear fuel used in FSU and European commercial power reactors. The range of the parameters is limited to specific data which are characteristic for origin and intended use of nuclear material. These are e.g. data from macroscopic parameters (i.e. fuel pellet dimensions), chemical and isotopic compositions, impurities (e.g. Fe, Cr, Ni, Al, Ca, Si, F, Cl) and roughness of the fuel pellet surface. At the

moment the databanks serve more for uranium origin determination, but new parameters like microstructure and morphological characteristics of powders (e.g. platelet and grain sizes), data of mixed oxide fuels in LWRs, and HEU and Pu in research reactors are planned to be included. This additional data can help in the origin determination of the plutonium.

3. Plutonium

Plutonium (Pu) is element 94 in the periodic table and is named after the planet Pluto. It is an artificial element that is produced in natural or slightly enriched uranium fuelled thermal nuclear reactors, in fast-breeder reactors or as a by-product in other reactors. The first synthesised plutonium ^{238}Pu was produced by the bombardment of uranium with deuterons in the cyclotron in the University of California, Berkeley in 1941 by Seaborg, McMillan, Kennedy and Wahl. ^{239}Pu was produced shortly thereafter by the capture in ^{238}U of neutrons produced by (d,n) reactions. Till now 16 plutonium isotopes (^{232}Pu-^{247}Pu) with certified half-lives have been produced [23]. Plutonium is valuable in nuclear reactors and nuclear weapons because neutrons of all energies induce fission in ^{239}Pu.

In nature plutonium occurs in uranium ores as a result of the capture in ^{238}U of neutrons of spontaneous fission and alpha-neutron reactions. The concentration of plutonium is, however, extremely minute, only the order of one part in 10^{11} of uranium present. Also trace amounts of ^{244}Pu, the longest living plutonium isotope, have been found in cerium ore as surviving remnants of plutonium present at the formation of the earth. Plutonium is a very radiotoxic element, because of high rate of emission of alpha particles. It normally exists in biological systems in the +4 oxidation state. As ingested Pu is rather harmless, because it is not absorbed in the gastrointestinal tract. However, inhaled Pu concentrates in bone, liver and kidneys, where its biological half-life is up to 100 years [24].

3.1 Reactor produced plutonium

In nuclear reactors, where uranium fuel is irradiated, plutonium isotopes of ^{238}Pu-^{242}Pu with smaller quantities of other isotopes (e.g. ^{236}Pu and ^{244}Pu) are produced. Pu isotopes are the result of neutron capture in ^{238}U and subsequent beta decays to ^{239}Pu that further captures neutrons as shown in Fig.2. ^{238}Pu has also an alternative route of formation from ^{235}U [26]:

$$^{235}U + n \longrightarrow {}^{236}U + n \longrightarrow {}^{237}U \xrightarrow{\beta^-} {}^{237}Np + n \longrightarrow {}^{238}Np \xrightarrow{\beta^-} {}^{238}Pu \qquad (14)$$

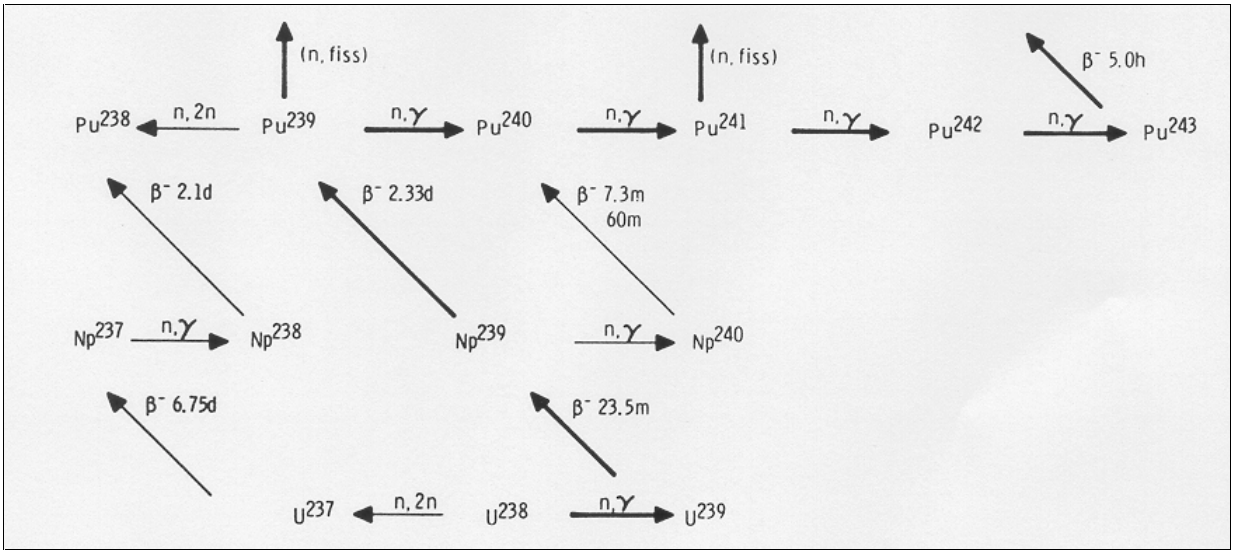

Fig.2. The production of plutonium from neutron irradiation of natural uranium [25].

Plutonium may be produced from ^{238}U in a reactor with any type of neutron spectrum, i.e. thermal or fast. A large variation in the plutonium composition is perceived as a result of differences in the average cross sections of the various isotopes over the different neutron spectra (Table 3). In general, more fissions per atom of plutonium occur in the fast spectrum than in the thermal spectrum. Thus plutonium formed in a fast reactor is predominantly ^{239}Pu, whereas significant quantities of the heavier isotopes are present in the plutonium from thermal reactors (LWR, HWR, Graphite Moderated Reactor). Among the thermal reactors, neutron moderator qualities decrease in the order of the used moderator D_2O > C > Be > H_2O resulting the softest (i.e. the most thermal) neutron spectrum in HWR [26]. Besides the moderator, also burn-up (i.e. power level times irradiation time), neutron flux and initial ^{235}U enrichment of the uranium fuel are reactor type specific and have an influence on the plutonium composition.

Table 3. The nuclear data of main Pu isotopes [23,26].

Isotope	$T_{1/2}$ (a)	Neutron capture cross section (b)	Fission cross section (b)	Neutron capture cross section (b)	Fission cross section (b)
		Thermal neutrons (0.025 eV)		Fast neutrons (1 MeV)	
^{238}Pu	87.74	510	17	-	-
^{239}Pu	2.411×10^4	270	752	0.04	1.73
^{240}Pu	6563	290	0.044	0.18	1.06
^{241}Pu	14.35	370	1010	2.0	1.56
^{242}Pu	3.750×10^5	19	< 0.2	-	-

Nuclear reactors can be divided in three categories depending on the purpose they serve. 1) Commercial reactors are used to produce electricity, 2) military reactors create materials for nuclear weapons, and 3) research reactors develop nuclear weapon or energy production technology, but additionally they are also used for training purposes, nuclear physics experimentation, and producing radioisotopes for medicine and research (Table 4).

Table 4. Main nuclear reactor types [26,27].

Reactor type	**Subtype**	**Chemical composition of the fuel**	**Enrichment**	**Moderator**	**Coolant**	**Purpose**
LWR	PWR	UO_2	low-enriched	H_2O	H_2O	electricity, nuclear powered ships
	BWR	UO_2	low-enriched	H_2O	H_2O	electricity
HWR	-	UO_2	nat. U or slightly-enriched	D_2O	D_2O	electricity, Pu production
Graphite Moderated Reactor	Gas cooled; Magnox	UO_2, UC_2 or metal	nat. U or slightly-enriched	graphite	CO_2 or He	electricity, Pu production
	Water cooled; RBMK	UO_2 or metal	Slightly-enriched	graphite	H_2O	electricity, Pu production
FBR	LMFBR	PuO_2/UO_2	Various mixtures of ^{239}Pu and ^{235}U	-	liq. Na	electricity, Pu production

3.2 Fissile Material Cut-off Treaty

Fissile Material Cut-off Treaty (FMCT) was proposed the first time already in 1956 by President Eisenhower, but it was rejected for decades due to the political situation between the USA and Russia. In 1993 President Clinton initiated the discussion again. This led to an agreement to begin negotiations on the FMCT at the Geneva Conference on Disarmament (CD) in 1995 [28].

The FMCT would strengthen nuclear non-proliferation norms by adding a binding international commitment to existing constraints on nuclear weapons-usable fissile material. The treaty would ban the production of fissile materials for nuclear weapons and other nuclear explosive devices. Even if the scope is limited, i.e. only a ban of future production, it must be ensured that material produced in the future is not falsely declared as earlier production. Therefore, all civilian and military materials produced after entry into force would need to be put under safeguards. However, this is not alone enough, but also a method is needed in the verification of the FMCT. There the age determination plays crucial role, because it is the only tool, which safeguards authorities have in order to verify the observance of law.

4. Isotopic correlation technique

The isotopic correlation technique (ICT) was developed on the 1970's in the framework of safeguards to verify the Pu-content of spent fuel assemblies. Later ICT was extended to verify the consistency of the isotopic analyses performed at the reprocessing plant input and to deduce the amount of specific isotopes in the fuel from measurement of other isotopes using established corrections. Correlations can be divided into three categories:

1) Correlations based on isotopes of heavy elements (^{235,236,238}U-, $^{238\text{-}242}$Pu-, ^{241,243}Am- and ^{242,244}Cm)
2) Correlations based on isotopes of stable fission products (^{83,84,86}Kr, ^{131,132,134,136}Xe, ^{143,145,146,148}Nd)
3) Correlations based on isotopes of radioactive fission products (^{106}Ru, ^{134,137}Cs, ^{144}Ce, ^{154}Eu)

The experimental data for the correlations was obtained using reprocessing data on oxide fuels from various reactors. Following correlations were established: Correlations between 1) two isotope ratios, 2) isotope content and isotope ratio, 3) two isotope contents, 4) isotope ratio or isotope content and fuel burn-up or ^{235}U depletion [29-31] (Fig.3).

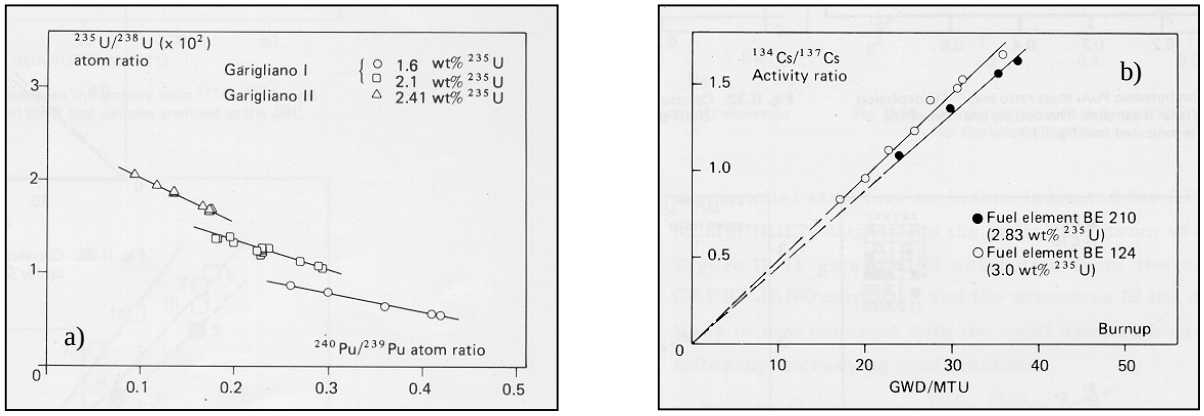

Fig.3. Examples of isotopic correlations a) $^{235}U/^{238}U$ vs. $^{240}Pu/^{239}Pu$ atom ratio, b) $^{134}Cs/^{137}Cs$ activity ratio vs. fuel burn-up [30].

4.1 Computer codes

Burn-up codes are used to compute the composition of the spent fuels. The most commonly used code is ORIGEN, which was written at ORNL [32]. A modified version from

ORIGEN, called KORIGEN has been developed at the FZK (German national research centre in Karlsruhe) to support more European reactor and fuel types [33]. In principle the burn-up codes solve the system of differential equations that describe the evolution of the isotopic vector, taking into account the radioactive decay and the neutron induced reactions. For this the codes need the decay modes with half-lives, the average cross sections of the neutron induced reactions and the neutron flux. The above-mentioned computer codes meet their most difficult problem in the values of cross sections, because these values are strongly dependent on the energy distribution of the neutron spectrum. The spectrum changes from a reactor to another, between different regions within the same reactor and with time due to the evolution of the fuel composition with the burn-up. The solution to these problems can be solved by computer codes such as SCALE, where the calculations are more realistic, but much more time consuming and complicated [34].

4.1.1 ORIGEN2

ORIGEN2 is a revision and update of the original ORIGEN computer code. It is a versatile point-depletion and radioactive decay code for use in simulating nuclear fuel cycles. The code calculates the composition and other related properties of nuclear materials and forms the basis for the study and design of fuel reprocessing plants, waste treatment and disposal facilities. It is also used for risk analyses calculations and support of nuclear power licensing and regulation.

ORIGEN2 databases contain in total 1700 nuclides divided into three categories: 130 actinides, 850 fission products and 720 activation products. The cross-section libraries cover the main commercial reactors and fuel types, such as uranium and U-Pu cycle PWRs and BWRs, thorium-based fuel PWRs, once-through uranium cycle CANDUs and U-Pu and thorium cycle LMFBRs. The structure of the input is simple and normally only a few changes have to be done to the standard input. The changing parameters are the libraries of reactor and fuel type, initial fuel composition, final burn-up, irradiation time and power level/neutron flux. A typical example of the input is presented in Appendix A. In the output, besides the isotopic composition, it is possible to obtain parameters like radioactivity (alpha and total), thermal power, neutron-induced fission and neutron absorption rate, (α,n)-reaction and spontaneous fission neutron production rate. Also parameters concerning the risk to health like chemical ingestion, radioactive ingestion and inhalation hazards can be obtained in the output [35,36].

4.1.2 SCALE

SCALE is not a single code, but a collection of several codes, each one performing different tasks with a standardised input/output system that allows one to enter automatically the output results of a module as input data for the following one. Normally, the so-called SAS2H sequence (Appendix B) is used to compute spent fuel composition. Although SCALE is more sophisticated than ORIGEN, still some assumptions have to be made in the calculations. The strongest assumption is that the described pin is considered as representative of the entire assembly. Thus, local effects such as corner pins or pins close to heterogeneities (e.g. absorbers, guide tubes, poisoned pins) can hardly be reproduced. The second limitation is that the SAS2H procedure can take into account just a single evolving composition and pins with different enrichment inside the same assembly must be treated either separately or mixed together by giving an average enrichment to the whole fuel assembly. A minor limitation is that full pellets have to be considered in the calculations because of the bad modelling in the pellets with central holes [34,37].

4.1.3 Accuracy of the computer code calculations

Verification of the composition predictions is a wide-ranging subject due to the large number of nuclides accommodated by the computer codes. The assumption is generally made that most of the fission products will be accurate if the actinide build-up and depletion are correct because they are heavily dependent on the fission yields, which are relatively well known. For this reason, verification efforts have been concentrated on the actinide region.

Regarding plutonium isotope calculations, comparisons between computer code calculations and experimental data have been made for ORIGEN2 and SCALE. ORIGEN2 calculations give reasonably accurate results for the main Pu isotopes, ^{239}Pu, ^{240}Pu and ^{241}Pu, in PWR, where the discrepancy is mainly within a few per cent. The isotopes ^{238}Pu and ^{242}Pu are, however, both consistently underestimated, having discrepancy close to 10 % [35]. The more extensive study of SCALE shows the same trend for all studied reactor types, i.e. PWR, PWR-MOX, BWR and Candu. However, it also points out the difficulties in BWR and PWR-MOX calculation, where the differences between calculated and experimental values of individual cases can be sometimes close to 30 % [37,38].

5. Mass spectrometric techniques

Thermal ionisation and secondary ion mass spectrometry are reviewed in a frame of their principles and peculiarities. The secondary ion mass spectrometry is used in this study as an analytical technique for particles, whereas the thermal ionisation mass spectrometry is considered as a technique for bulk analyses. However, a possibility to analyse particles by thermal ionisation mass spectrometry is not excluded.

5.1 Thermal ionisation mass spectrometry

Thermal Ionisation Mass Spectrometry (TIMS) is a well-recognised technique for the precise and accurate determination of isotope ratios of the elements with low ionisation potentials. Coupled with Isotope Dilution (ID-TIMS), the technique can be used to determine the concentrations of elements present in a variety of matrices. TIMS is a single element and at the most an oligoelement technique due to different ionisation energies and vapour pressures of the elements and molecules. It can be used for the analyses of actinides, lanthanides, alkalis and alkaline earth elements and it has been found to be a very powerful technique in nuclear technology, geochronology and life sciences.

5.1.1 Principle

The principle of TIMS is shown in Fig.4. A sample as a solution of a salt (e.g. nitrate, chloride) or an oxide, containing amounts varying between pg and μg of the element of interest, is placed on a high purity filament assembly and dried. In an ion source the sample is evaporated, ionised and accelerated. A mass analyser separates the ions according to their mass to charge ratios (i.e. m/z values), which for the magnet analyser is followed by the law:

$$m/z = r^2H^2/2V, \qquad (15)$$

where r is the radius of curvature of the ions, H is the magnetic field and V is the acceleration voltage [39]. The resolved ion beam is collected finally by the detector.

Requirements for the efficient thermal ionisation of the formation of positive ions are: high work function of the filament material and low ionisation potential of the determined element. Due

to their high work function and high melting point, rhenium, tantalum and tungsten are the mostly used filament materials in positive thermal ionisation (PTI). Recently also negative thermal ionisation (NTI) has been used for isotope ratio determination of some metal oxides and non-metals with high ionisation potential. In this case a filament material with low work function, like thoriated tungsten, is used [40].

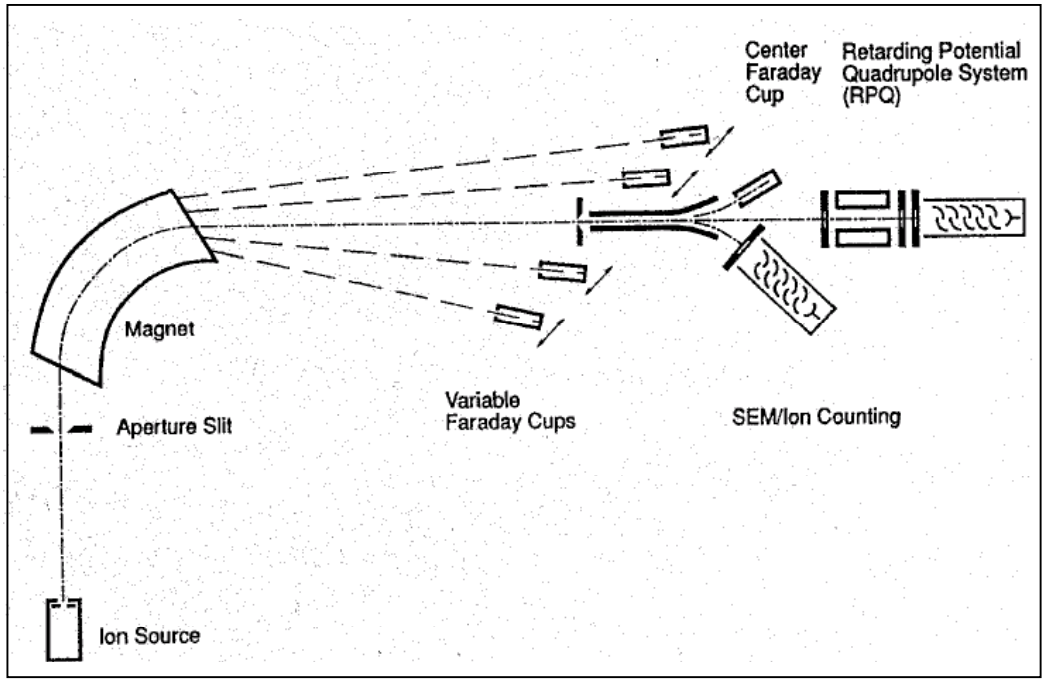

Fig.4. TIMS with extended geometry and multi Faraday cup detector system [39].

5.1.2 Instrumentation

5.1.2.1 Ion source

All commercial thermal ionisation sources are equipped with rotating sample magazines (turrets), where up to 21 filament holders can be loaded. Single, double or triple filament assemblies can be used. Double and triple filament assemblies are favourable compared to single filament, because the evaporation and ionisation conditions are easier to control with separate filaments. The formation of positive ions in the thermal ionisation source is governed by the Langmuir equation:

$$n^+/n_0 \propto \exp(\Phi\text{-}I)/kT \qquad (16)$$

where n_0 and n^+ represent the number of neutral atoms/molecules and the number of positive ions leaving the filament, respectively, Φ is the work function of the filament material, I is the first

ionisation potential of the element, k is the Boltzmann constant and T is the temperature of the filament [39].

In the double filament assembly, the sample is evaporated on the evaporation filament, in which the atoms and molecules come loose. The atoms/molecules draw close to the ionisation filament, where they are ionised by losing an electron (or in NTI gaining an electron). In triple filament assembly, the sample is placed on two side filaments, while the central filament acts as the ionisation filament. This arrangement can be used to compare two different samples (e.g. a standard and an unknown sample) under the same ion source conditions. The positive ion beam is then accelerated and focused in the collimator with several lenses by applying a potential (Fig.5). A variety of specially prepared filament surfaces are employed in TIMS with the objective of improving the ionisation efficiency especially for single filament measurements, controlling the rate of evaporation or maximising the yield of production of a particular ion [41-48].

The sensitivity of a thermal ion source is usually given by the number of sample atoms evaporated from one of the filaments in order to produce one ion at the output of the mass spectrometer. Typical values are from 5 % for Pb in a single filament silica gel environment down to less than 0.01 % for Hf in a triple filament source. All other important elements, such as U and Pu, range between these limits [40].

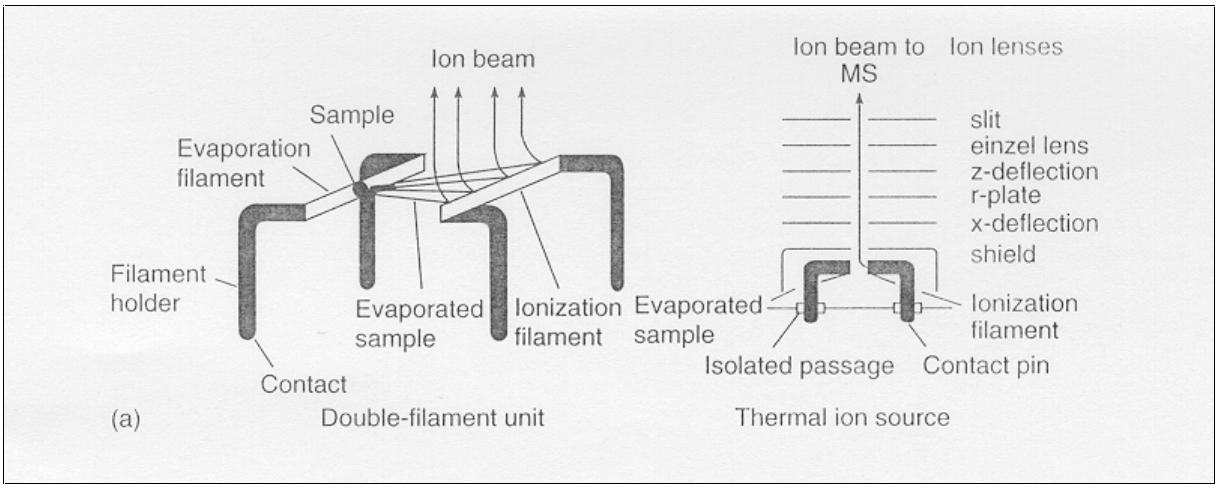

Fig.5. Schematic diagram of a double filament thermal ionisation ion source [40].

5.1.2.2 Mass analysers

The mass analyser separates ions according to their mass-to-charge ratio. The main types of mass analysers used in mass spectrometry include magnetic sector, quadrupole, time-of-flight (TOF) and Fourier transform ion cyclotron resonance. Conventionally, the single stage magnetic

sector analyser has been used for mass separation in TIMS, because the ions formed in the thermal ionisation source have only thermal energies and their energy spread is small (0.1 to 0.2 eV). The 90° magnetic sector has been found to be a useful configuration in many commercial instruments and it has displaced the older 180° and 60° sectors. In normal geometry, the central path of the ion beam is perpendicular to the magnetic analyser at the entrance and the exit. When the extended geometry is used (Fig.4), the ions are allowed to enter and leave the magnetic analyser at oblique incidence angle 26.5°. This configuration focuses the ion beam in the Z-direction and doubles the dispersion of the ions in the magnetic field with the same radius of curvature compared to normal geometry. Therefore the resolution of the mass spectrometer is improved and resolution between 400-500 (defined as M/ΔM at 10 % valley) is reached [39,49].

5.1.2.3 Detection

Mass separated ions are collected by a detector. Four detector types are used in TIMS: Faraday cup, Secondary Electron Multiplier (SEM), Daly detector and Channel Electron Multiplier (Channeltron). The Faraday cup is used when sufficient ion current is available to obtain electric current in a range of 10^{-14}–10^{-10} A. For measuring small ion currents or very low abundant isotopes, i.e. currents from 10^{-18} to 10^{-13} A, SEM, Daly and Channeltron are used.

The Faraday cup serves as a source for charge compensating electrons when measuring positive ions (or as a sink in the case of negative ions). These electrons are then measured as an ordinary electric current. This is achieved by feeding the electron current through a high ohmic resistor, typically 10^{11} Ω, and by measuring the voltage across this resistor. The inner surface of the Faraday cup is coated with a material of low sputter rate, e.g. porous carbon and the width to length ratio of the cup is made as small as possible, to prevent reflected or sputtered particles leaving the cup. After many years of using just single collector system, recently multi-collection with Faraday cup has become favourable and up to 9 isotopes can be measured at the same time. This makes it possible to achieve an internal precision of 0.001 % on isotope ratios [40].

In SEM the collected ions hit the ion-electron conversion dynode, which releases electrons. The electrons are accelerated to the following electron-electron dynode, and typically 10-16 dynodes one after the other are used. Between each of the dynode, several hundred volts acceleration voltage is applied to reach finally amplification factor of about 10^8 for an ion. SEM can be used in two modes: analog (i.e. measuring current) or pulse counting mode. The advantage of the SEM used in analog mode is its high sensitivity, but as a disadvantage it has poor precision

due to the variable amplification factor, which depends on the mass of the measured ion. When using SEM in pulse counting mode, it is inherently noiseless and only rarely may electrons be produced by field effect tunnelling or by cosmic rays, resulting a dark noise rate of only few counts per minute. However, at high count rates the linearity suffers due to the dead time effect [40,49].

Before SEM, a somewhat different ion-counting device, a Daly detector was presented. Ions are accelerated by 20-40 kV to a secondary-emitting electrode. The realised secondary electrons are accelerated by the same electrostatic field to hit a grounded scintillator. There they are converted to photons, which are then detected by an ordinary photomultiplier. Except for a slightly higher dark noise value for Daly, the two detector types (SEM and Daly) do not differ in the quality of the ion counting [40,49].

During the last few years, a new kind of ion-counting detector, the Channeltron, has become available. The Channeltron consist of a ceramic body with a small, curved, interior channel (Fig.6). The inside wall is coated with a thin layer of high resistance lead oxide. A negative high voltage (~2000 V) is applied on the entrance to generate an avalanche of electrons for each entering ion. The biggest advantage of the Channeltrons, compared to other ion-counting detectors, is their compact size, which gives the possibility to replace the Faraday cups by them and measure low ion currents by multi-collection. A disadvantage is the variable amplification factor caused by different points on the entry where the ions hit [49,50].

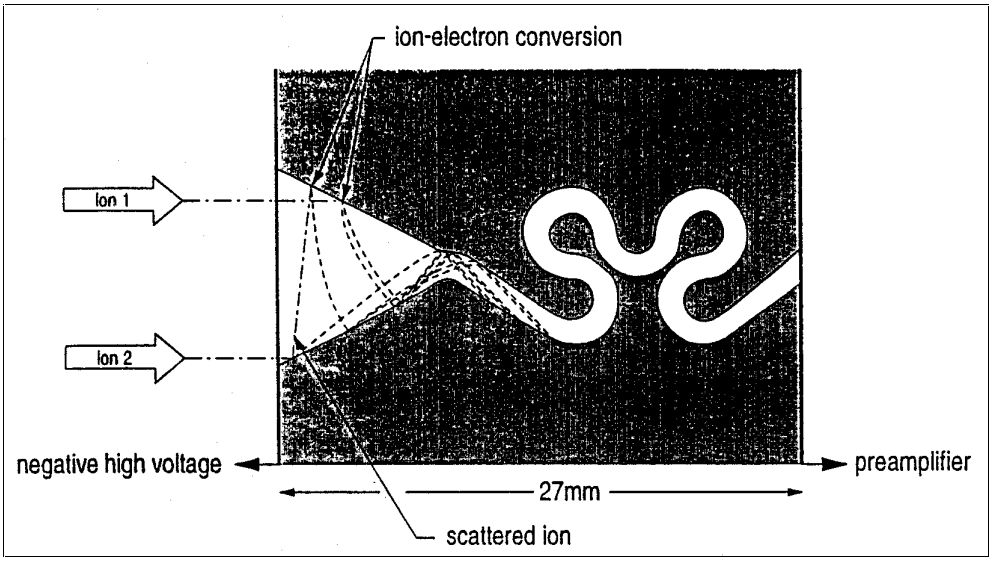

Fig.6. Schematic diagram of a Channeltron [50].

5.1.3 Isotope ratio measurements

Isotopic ratios measured with a thermal ionisation mass spectrometer are seldom the "true" ratios of a sample under study. Many factors have to be taken into account, among these being the effects arising from the instrumental parameters; these are taken care of through calibration (Chapter 5.1.3.1). Effect arising from the measurement process itself is essentially isotopic fractionation (Chapter 5.1.3.2). Afterwards the expected atom ratio ($R^{i/j}_{(corrected)}$) can be calculated as follows:

$$R^{i/j}_{(corrected)} = \frac{R_{(measured)}}{(Gain)_{i/j} \times (CF)_{i/j}} \times \left[1 + B \times (j - i)\right] \qquad (17)$$

where $(Gain)_{i/j}$ is the relative gain ratio of the amplifiers used to measure isotopes i and j, $(CF)_{i/j}$ is the relative Faraday cup efficiency factor, B is the isotopic fractionation factor per atomic mass unit $(1/(j\text{-}i) \times (R^{i/j}_{true} / R^{i/j}_{obs} - 1))$ and (j-i) is the atomic mass difference of the measured isotopes [51].

5.1.3.1 Calibration

The calibration procedure depends on the measurement mode that is going to be performed i.e. peak jumping (dynamic) or multi-collection (static). In peak jumping, a single detector is used and by switching the magnetic field, isotopes in question are measured subsequently. The calibration in this case is very simple, requiring only the mass calibration (called also the magnet calibration). The full-scale mass calibration is performed normally using the isotopes ^{23}Na, ^{41}K, ^{185}Re, ^{187}Re, ^{238}U and ^{244}Pu.

When measuring by the multi-collection mode (i.e. isotopes are measured simultaneously with an array of detectors), more calibration parameters have to be considered. This is caused by the detectors, which may vary with respect to their geometry, construction and component materials. Detectors calibration against each other includes gain calibration, cup efficiency calibration, linearity check and, in a case of different detector types, normalisation between them. Collectors have to be set also on the right positions on the focal axis, so that all the isotopes are collected in the each collector from the centre of the flat-top peak.

In gain calibration the amplifiers of the adjustable Faraday cups are calibrated against the amplifier of the fixed Faraday cup by applying the ground potential and constant signal of 9V to all amplifiers one by one. Later the gain per volt is calculated and stored in the software [51].

Cup efficiency calibration checks the response of stable ion beam in the Faraday cups, which should be near unity. Cup efficiency factor (CF) can be determined using either peak-shift or peak-jump experiments. In the peak-shift experiment, isotopes can be placed into different detectors by moving the mass spectrum to the high or low mass side in increments of one mass unit. The CF is then calculated from the isotope ratios measured with different configurations. The peak-jump experiment selects a stable ion beam of single isotope to measure ion intensities in each movable detector and a reference detector with symmetrical scanning sequence. The peak-jump experiment is favourable over the peak-shift experiment because 1) no fractionation is involved for a single isotope, 2) no dependency on different isotopes, 3) direct comparison between detectors, 4) applicable to any detector configuration, and 5) the same magnitude of ion intensities is measured in each detector. However, if the signal is not very stable, there occur time dependent effects. Thus the measurement sequence has to be symmetrical. The CF values have been noticed to be independent of the measured element for Faraday cups, however the magnitude of the ion intensities can affect the CF values, thus the calibration should be performed using the same ion intensity level as later in the sample measurements [51,52].

The linearity of the detectors can be check by measuring the IRMM 072 reference materials with $^{233}U/^{235}U$ atom ratios ranging between 1 and 2×10^{-6}, $^{235}U/^{238}U$ ratios being near unity. The ^{233}U, ^{235}U and ^{238}U isotopes are measured in each detector using peak jumping mode. The linearity factor of cup (x) is then given by:

$$LF_{(x)} = \frac{R'_{3/5}}{R^{c}_{3/5}} \tag{18}$$

where $R^{c}_{3/5}$ is the certified $^{233}U/^{235}U$ ratio, $R'_{3/5} = R_{3/5} \times (1 + 2 \times B)$, $B = (K-1)/3$, and $K = R^{c}_{5/8}/R_{5/8}$ [51].

When using ion counting detectors (SEM, Daly or Channeltron) together with Faraday, the detectors have to be calibrated against each other to determine the detector efficiency factor (DEF). This is performed by sending reasonable low and stable ion beam to a Faraday cup and then to Daly or SEM (peak-jump experiment). After this, the Channeltrons need still to be calibrated against SEM or Daly with same procedure.

5.1.3.2 Fractionation

Fractionation is a phenomenon that is induced by the mass dependent differential evaporation of the isotopes from the heated sample filament. This difference causes the lighter isotope to evaporate more rapidly from the evaporation filament. The fractionation is based on the Rayleigh's distillation law, where the rate of evaporation is proportional to $1/\sqrt{m}$.

During the evaporation process, the higher evaporation rate of the lighter isotope leads to faster depletion of the sample in this isotope and the observed ratio of light to heavy isotope decreases towards its true value and, eventually, below it. Parameters, which affect the mass fractionation are: sample size, chemical composition and purity of the sample, sample loading procedures on the filament, the material of the ionisation and evaporation filaments, filament temperatures, the rate of sample heating and the time of data acquisition [53].

Many models and techniques to correct for fractionation have been developed [54,55]. The major difficulty to develop a general quantitative fractionation model is the lack of reliable or appropriate thermodynamic data on the evaporation and ionisation species under the non-equilibrium conditions in the thermal ionisation source. The following expressions are typically used to correct the mass discrimination [40]:

- Linear law: $R_{tr}/R_{meas} = 1 + \Delta m \times \varepsilon_{lin}$ (19)
- Power law : $R_{tr}/R_{meas} = (1 + \varepsilon_{pow})^{\Delta m}$ (20)
- Exponential law: $R_{tr}/R_{meas} = \exp(\Delta m \times \varepsilon_{\exp})$ (21)

where R is the ratio of the heavier isotope m_1 to the lighter isotope m_2, ε is the mass bias per atomic mass unit, and $\Delta m = m_1 - m_2$. In the case of U and Pu analysis, normally the linear approach is sufficient (as in eq. 17), because of relative small mass differences and high mass numbers of the elements leading to the R_{tr}/R_{meas} ratio near unity.

Experimental K-factors, i.e. certified isotope ratio/observed isotope ratio, have also been determined to correct the fractionation [53,56]. From the K-factor, a mass discrimination factor (mdf) per mass unit can be calculated. It has been noticed that K-factors depend mostly on the sample amount, thus it is not constant for an element of different sample sizes. It has been observed the K-factor being unity, when ≈ 63 % of the sample is consumed [57]. Thus the data for K-factor determination should be collected from the same segment of the isotopic fractionation curve, which is virtually impossible.

"Double spiking", called also as an internal standard method, is a correction technique, where a pure and calibrated mixture of spike isotopes (e.g. ^{233}U and ^{236}U) in approximately equal amounts is mixed with an unknown sample. For example, in a case of uranium, the $^{233}U/^{236}U$ and $^{235}U/^{238}U$ ratios are determined and a correction factor, $(^{233}U/^{236}U)_{meas}/(^{233}U/^{236}U)_{tr}$, is established and used to correct the measured $^{235}U/^{238}U$ ratio [58,59].

In the internal normalisation technique, it is assumed that the element under study has three or more isotopes and that at least two of them are stable isotopes, whose ratio in nature is unaltered. Such a pair of isotopes has a constant, well-established isotopic ratio and it may be used for mass discrimination corrections. This technique is widely used e.g. in strontium and neodymium isotope ratio determinations.

5.1.3.3 Total evaporation

The total evaporation technique is the latest application in thermal ionisation mass spectrometry. It was described for the first time in 1987 [60]. A salient feature of the technique is the evaporation of the entire sample while simultaneously integrating the signal of each interested isotope by multi-collection. Thus virtually, by this technique, the fractionation problem has been eliminated. Also the amount of sample has been reduced considerably (from μg to ng) because the stable ion beam is no longer required and the analysis time is only a few minutes. The potential advantages of the total evaporation method are higher accuracy and precision, which have shown an improving factor of 2 to 4 comparing to the conventional method [61]. It is also less dependent on the sample preparation chemistry and the sample amount on the filament can vary at least by a factor of 20 without showing any significant bias. Different filament materials have been noticed to affect the results. Tantalum filaments are unsuitable because of incomplete sample consumption during the analysis from the filament. Additionally, and due to that, the isotope ratios are positively biased. Rhenium and tungsten materials did not show these problems [61-63]. A major disadvantage of the total evaporation technique is that isobars can not be separated by altering evaporation conditions. However, in some cases this can be performed by deconvoluting the contributions from two elements to a mass, because each element has a different evaporation curve [64].

5.1.4 Isotope dilution analysis

Isotope dilution analysis (IDA) is a quantitative determination technique to determine the concentration of the element in the sample. The technique can be applied to the elements, which have at least two stable or long-lived radioactive isotopes [65]. The principle of the IDA is to compare an unknown number (N_X) of atoms of an isotope to a known number (N_Y) of atoms of a non-present but added isotope of the same element (called spike) through a measurement of a ratio of numbers of atoms (R_B) of two isotopes (Fig.7):

$$N_X / N_Y = R_B \tag{22}$$

The general IDA equation of multi-isotopes is defined:

$$N_X / N_Y = \frac{R_Y - R_B}{R_B - R_X} \times \frac{\sum R_{iX}}{\sum R_{iY}} \tag{23}$$

where R_X, R_Y and R_B are the isotope abundance ratios of two interested isotopes in sample, spike and blend, respectively [66]. The net change in the isotopic composition of the sample is not only dependent on the contrast of its isotopic composition with that of the spike but also on the relative amounts of the sample and tracer elements in the blend. Due to that, the concentration and composition of the spike, as well as the weight, must be known accurately. It is necessary to ensure that all the isotopes of the element are in the same valence state after mixing the sample and spike solutions, in other words, they have to be in chemical equilibrium. The sample has to go usually through a chemical separation to obtain pure and isobaric interference free sample for the isotope ratio measurements. An attractive feature of the IDA is that after the mixing of the sample with the spike, the chemical separation of the blend does not have to be quantitative, because isotopic ratios are measured.

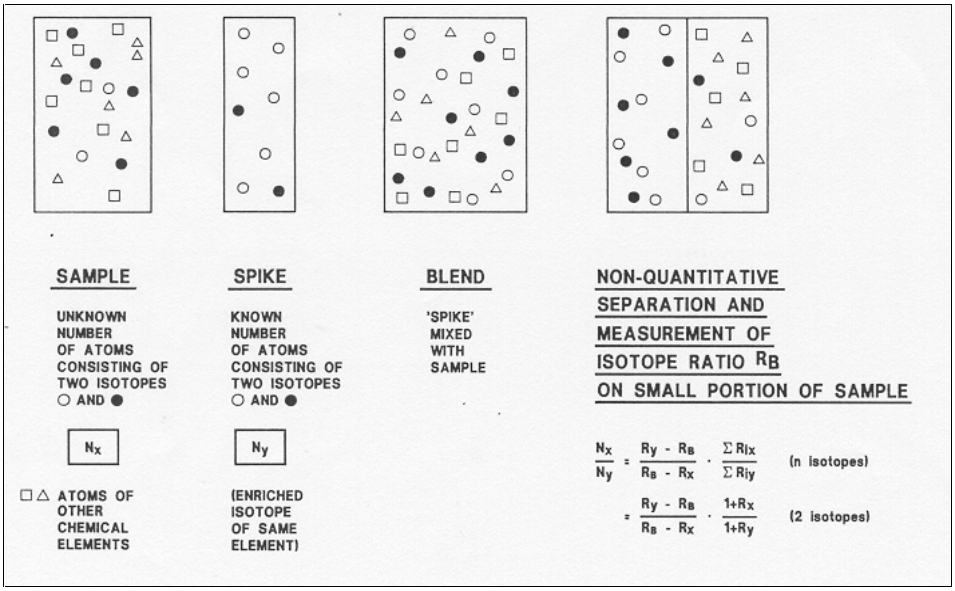

Fig.7. Principle of isotope dilution analysis [66].

5.2 Secondary ion mass spectrometry

Secondary ion mass spectrometry (SIMS) is a technique used mainly for the characterisation of materials in fields of the semiconductor, metallurgy, geology, organic and biology [67,68]. Nowadays it has been found to be also a powerful tool in the particle analyses [69,70]. SIMS has many advantages compared to other surface techniques, e.g. low detection limits (ppm to ppb), all elements are detectable, isotopes distinguishable and insulators analysable. On the other hand it has disadvantages like the element and matrix dependent secondary ion yields and the isobaric mass interferences.

5.2.1 Principle

Secondary ion mass spectrometry is an analytical technique that can be used to characterise the surface and near surface (~ 30 μm) region of solids and some liquids. The technique uses an energetic primary ion beam (0.5-20 keV), which impact triggers off cascades of atomic collisions, some of which end up in the ejection of one or several atoms belonging to the most superficial layers of the sample. Many species (e.g. single and multiple charged ions, clusters of several atoms and neutrals) are formed by the interaction of the beam with the sample, but the positive and negative ions are the species of interest for SIMS. The sputtered secondary ions supply information about the elemental, isotopic and molecular composition of the material, and they are detected by a mass spectrometer (Fig.8).

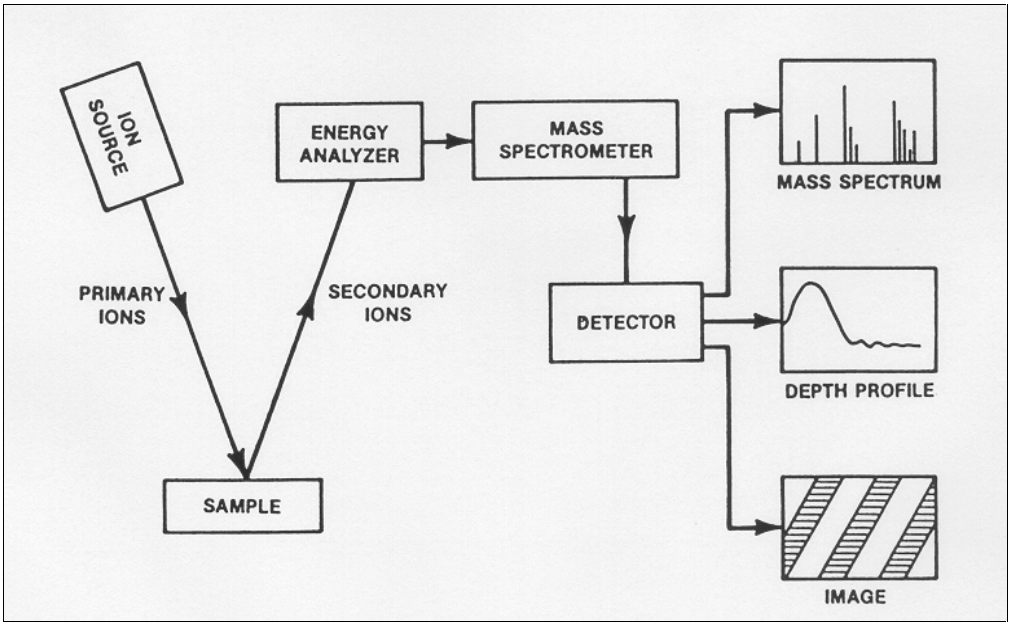

Fig.8. SIMS technique block diagram [71].

5.2.2 Instrumentation

5.2.2.1 Primary ion source

The primary ion beam is generated in the primary ion source. The choice of the primary ion beam depends on the elements to be analysed and the type of information required. The selection of a certain primary beam affects secondary ion yields, detection limits, depth resolution, lateral resolution, charge neutralisation, microtopography formation, and sputtering rates. The commonly used primary beam species are O_2^+, O^-, Cs^+, Ar^+, Xe^+ and Ga^+, where O_2^+ and Cs^+ are the most typically used for the detection of electropositive and negative species, respectively, due to their ion yield enhancement capability.

Duoplasmatron ion source is the standard type of primary ion source used with ion microprobe instruments. In duoplasmatron, the gas (normally Ar or O) is fed to the interior of the hollow cathode through an adjustable leak. In the hollow cathode, a plasma is produced by an arc maintained between hollow cathode and anode. Ions are extracted from the plasma by a strong electrostatic field produced by an extraction electrode. The duoplasmatron can furnish positive or negative ions according to the polarity of the extraction potential [72].

Surface ionisation sources, Cs^+ and I^-, are used normally for two reasons: 1) to increase the secondary ion yields of electronegative and positive elements, respectively and 2) to obtain smaller beam size compared to the duoplasmatron source. Surface ionisation is based on electron

exchange between the conduction band of the metal and the ground state energy level of atom's valence electron. For example, in vapour state caesium ionises into positive ions when it comes into contact with the surface of a tungsten plate at a temperature of 1100 °C. The Cs^+ ions are extracted and accelerated by applying an electric field between the tungsten plate and the extraction electrode [72,73].

5.2.2.2 Secondary ion analyser

The loosened secondary ions are extracted by electric fields and energy and mass analysed. Depending on the analytical application, different kind of m/z analysers can be applied to perform the mass separation. In the first generation of SIMS, magnetic sector analysers were used. Later on, double-focusing, quadrupole and time-of-flight (TOF) analysers have been applied.

In double focusing spectrometers, a suitable combination of electrostatic and magnetic fields is used to obtain directional focusing of a given mass-to-charge ratio ion beam, even with heterogeneous energies (Fig.9). The secondary ion energy distribution from a sample varies with ion species. These energy differences can be used to simplify the mass spectra. Because molecular ions in general have a narrower energy distribution than atomic ions, an energy window can be used to select an energy portion of the interested species.

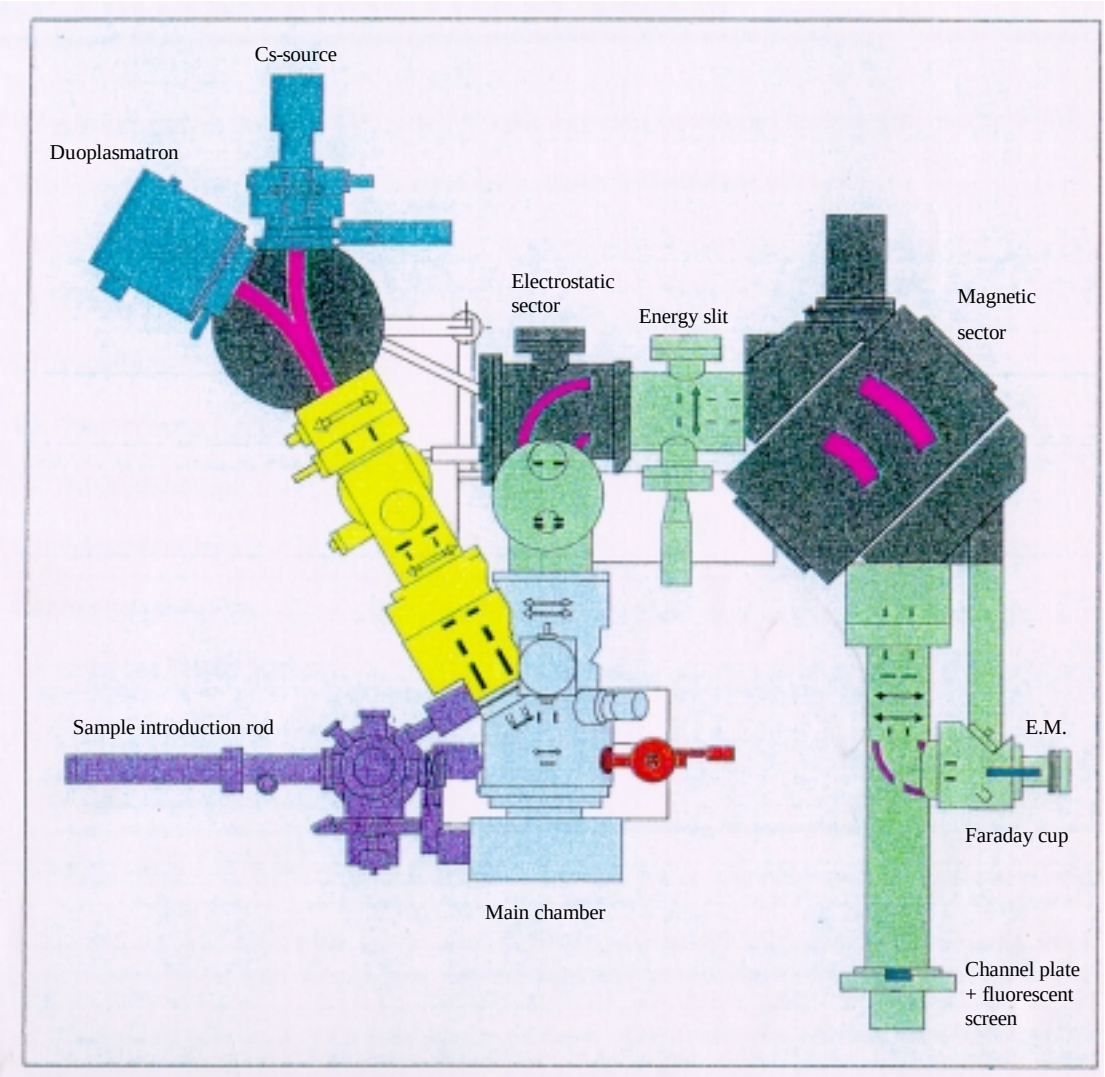

Fig.9. Double-focusing SIMS (Cameca IMS 6F) [73].

The quadrupole is actually a mass filter rather than an analyser because it transmit ions having only a small range of m/z values and moreover there is no mass dispersion or focusing as in magnetic analysers. Radio frequency (RF) and direct current (DC) electric fields are applied to a quadrupole rod structure and one is varied to produce a mass spectrum. Because quadrupoles do not employ magnets, peak switching for selected ion monitoring can be done quickly, which makes them ideal for depth profiling application [71].

Time-of-flight analysers are used with secondary ion beams that are generated in short pulses. Ions are accelerated into a drift tube in which the ions are separated according to the time taken to traverse the drift space. When ions have the same energy, heavier ions take longer to reach the detector than do lighter ones. TOF systems represent an area for organic materials and it is preferred for surface analysis, cluster studies and molecular structure elucidation because of its

virtually unlimited mass range, high mass resolution and ability to detect ions of different masses simultaneously [71].

5.2.2.3 Detection

The detection of the secondary ions can be done either by counting the ions (electron multiplier or Faraday cup) or using ion sensitive imaging detectors (microchannel plate/Fluorescent screen or resistive anode encoder). The principle of Faraday cup and electron multiplier has been explained before (Chapter 5.1.2.3), thus here is concentrated only on the imaging.

In ion imaging, the SIMS provides a spatial distribution of selected surface chemical constituent. In combination with depth profiling, 3-dimensional concentration maps can be generated. The MCP/FS system consists of a microchannel plate device coupled to a fluorescent screen. The MCP is an assembly of small channels. Each channel is a small hollow glass tube with the inner surface coated with SiO_2. When secondary ions strike the semiconductor surface, it causes a secondary electron emission. The electrons are accelerated and multiplied by collision cascades in the channel. The FS converts electrons in photons.

The RAE system consists also of a microchannel plate, but coupled to a resistive anode encoder system. The RAE generates a pulse for each secondary ion incoming on the channel plate and determines the spatial position of the gravity centre of the charges deposited by the electron flux by sharing the charge between its four corners [73]. RAE is used for the mapping of the entire sample surface.

Imaging can be done by two divergent ways, in ion microscope and ion microprobe mode. When measuring with the ion microscope mode, the sample is illuminated by a large-diameter primary ion beam so that each point of the surface may be considered as a source of secondary ions. A magnified image of the emission current density distribution of a selected secondary ion species, present at the sample surface, is produced on a scintillator screen. In ion microprobe mode, called also as Scanning Ion Image (SII), the secondary ion image is produced by a narrow illuminating ion beam, which is focused down to a small spot and rastered onto the sample surface. Synchronously, the mass-analysed secondary ion image is formed on the cathode ray tube (CRT) of the chassis by modulating the brightness of the spot as a function of the secondary ion intensities at each position of the primary beam [72].

5.2.3 Measurements

SIMS analyses can be divided into two categories, static and dynamic, depending on the information obtained. In static SIMS the molecular information on the composition of the uppermost monolayer is derived, without disturbing its composition and structure, when the primary ion beam intensity is kept below 10^{12} ions/cm^2. As the amount of matter that is sputtered is limited, and consequently the secondary ion yield low, TOF mass analyser has been normally chosen for static SIMS. The application is used for determination of the chemical composition of the metals, semiconductors, plastics, biomolecules, polymers and organic materials.

In dynamic SIMS, the primary ion beam intensity is not limited and the surface erosion is more violent and faster. Thus the supplied information is elemental and originates from deeper layers of the bombarded sample. One of the main applications of the dynamic SIMS is the analysis of trace elements depth distribution (e.g. dopants in semiconductors).

5.2.3.1 Matrix effect

Matrix effect is a general term used to describe differences in sensitivity for a given element in samples of different composition. Secondary ion yields for different elements can differ by over six orders of magnitude, and they can also vary from matrix to matrix. The emitted atomic or molecular particles have so-called charge states, which depend strongly on the chemical environment of the sputtered species. By changing this chemical environment, for example, going from a pure metal to an oxide, the ionisation probability of the same species, for example, a metal atom may be changed. The use of relative sensitivity factors (RSFs) can compensate the matrix effects when SIMS data are processed. The RSF takes into account the differences in sputtering rate and is a relative measure of the ionisation probability of a given element in a given matrix [71].

5.2.3.2 Mass interferences

Mass interferences are common in SIMS because of the variety and intensity of the molecular ions and the multiply charged species. Interferences can cause problems especially when the matrix has more than one element, the matrix elements have more than one isotope or several naturally occurring isotopes are of significant intensity. To solve the mass interferences, a few techniques can be applied. Firstly, the difference in energy distributions between atomic and

molecular ions can be used to advantage, because atomic ions have a broader energy distribution and an offset voltage can be used to discriminate the molecular ions. Secondly, high mass resolution (m/Δm) can be used to separate two ions with the same nominal mass (m), but with small difference of exact mass (Δm). Magnetic sector SIMS can typically offer mass resolution of 10000, where quadrupole instruments are limited to 500. Thirdly, molecular ion or isotope based interference subtraction can be used. In this technique, two naturally occurring isotopes of same element (or an atomic ion and a molecular ion) are monitored in a profile and any difference in normalised isotope profiles can be used to subtract the interference [71].

6. Results and discussion

6.1 Age determination

Age determination of Pu material was divided in two parts depending on the sample size. 1) Bulk samples (grams of material) were analysed by ID-TIMS after elemental separation (Pu/U/Am) and by gamma-spectrometry without separation [I]. Additionally the samples were analysed by ICP-MS (Chapter 6.1.3). 2) Particle samples were analysed by SIMS [II]. Because the particles are solids and very small of size (1 µm particle ≈ 10 pg), no preliminary treatment (i.e separation and purification) could be performed for the samples.

To determine the ages of Pu, individual parent/daughter ratios were calculated using the Nuclides 2000 program (Fig.10) [74].

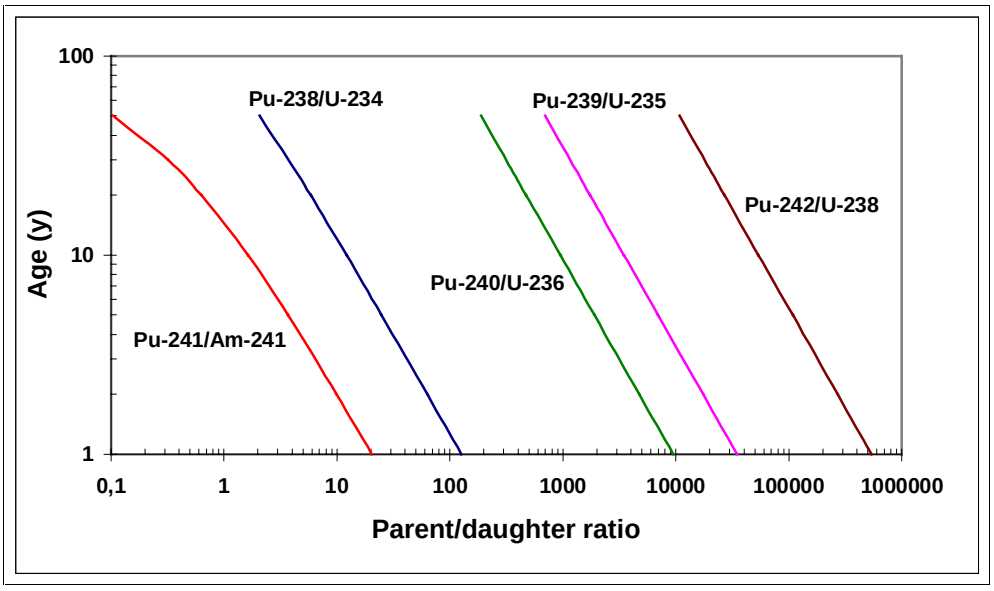

Fig.10. Age vs. parent/daughter atom ratios.

When curve fittings are made, the following equations are obtained:

$^{238}Pu/^{234}U$: $y = 105.38\ x^{-0.9563}$ (24)

$^{239}Pu/^{235}U$: $y = 34755\ x^{-0.9998}$ (25)

$^{240}Pu/^{236}U$: $y = 9427.1\ x^{-0.9994}$ (26)

$^{241}Pu/^{241}Am$: $y = 14.473\ x^{-0.8675}$ (27)

$^{242}Pu/^{238}U$: $y = 539167\ x^{-1}$. (28)

The curve fitting for the $^{241}Pu/^{241}Am$ ratio is valid only till ~20 a, because later the curve start to bend due to the short half-live of the ^{241}Pu and no good fit is possible to attain. The age can be calculated, however, always from the general decay equation. Because the half-lives of the daughter nuclides are long in the considered time range, their decay can be ignored. Thus the following equations can be used:

$$Pu_t = Pu_0 \times e^{-\lambda t} \tag{29}$$

$$Am_t = Pu_0 - Pu_t = Pu_0 \times (1 - e^{-\lambda t}) \tag{30}$$

$$R_{Pu/Am} = \frac{e^{-\lambda t}}{1 - e^{-\lambda t}} \quad \Leftrightarrow \quad t = \frac{1}{\lambda} \ln \frac{1+R}{R} \tag{31}$$

where Pu_t/Am_t is the number of Pu/Am atoms after the time t, Pu_0 is the number of Pu atoms in the beginning and λ is the decay constant.
These equations are, of course, valid for all the parent/daughter relations under consideration.

As a matter of practice in mass spectrometric age determination, the $^{242}Pu/^{238}U$ ratio is left out. This is due to the long half-live of ^{242}Pu, which leads only to a minute amount of in-growing ^{238}U. Additionally small U contamination can affect drastically the result of this ratio because ^{238}U is the most abundant U isotope both in natural and LWR fuel. In mass spectrometry analysis the isobaric interference between ^{238}Pu and ^{238}U also prevents the possibility to determine the age from the $^{242}Pu/^{238}U$ ratio, if the U/Pu separation before analysis has not been complete, which is often the case.

The measured Pu/U or Pu/Am ratios are inserted in the individual parent/daughter equations obtained from the Fig.10 and the ages are calculated. The ages from each individual equation should be, of course, in agreement. However, sometimes inconsistencies appear, which are normally due to:

1) Am leftovers after reprocessing. This causes higher age from the $^{241}Pu/^{241}Am$ ratio compared to the ages from the Pu/U ratios.
2) U leftovers after reprocessing or U contamination. This causes higher ages from the $^{239}Pu/^{235}U$ (and especially from the $^{242}Pu/^{238}U$) ratio. In the particle analysis it causes too low age from the $^{238}Pu/^{234}U$ ratio due to the isobaric interference of ^{238}U.

The multiple age determination (i.e. a few parent/daughter relations) is essential in order to be sure about the validity of the age. This is not only used to exclude the effect of daughter leftovers from reprocessing, but also to address the potential spoofing by the perpetrators who mix different materials. The mixture of two Pu materials of different ages gives various results as seen in Table 5.

Table 5. Variations in calculated ages when mixing after reprocessing two different Pu materials of different ages. Calculations were performed with Nuclides 2000 [74].

Sample	Initial composition				
	^{238}Pu	^{239}Pu	^{240}Pu	^{241}Pu	^{242}Pu
RR	1,9	57,0	26,3	8,2	6,7
R2	0,01	95,0	4,7	0,3	0,01
Mixture		Age			
		$^{238}Pu/^{234}U$	$^{239}Pu/^{235}U$	$^{240}Pu/^{236}U$	$^{241}Pu/^{241}Am$
70% RR 2a +	30% R2 30a	2,06	13,67	3,99	2,22
70% RR 30a	+ 30% R2 2a	29,77	18,33	28,00	28,52

6.1.1 Thermal Ionisation Mass Spectrometry (TIMS)

Four samples were analysed. SRM 946 and SRM 947 are $PuSO_4 \cdot 4\ H_2O$ isotope standard reference materials from National Institute of Standards and Technology, NIST, (formerly National Bureau of Standards). R1 and R2 were originally Pu-metal pellets, but which were oxidised during the years forming Pu oxide powders. The samples were spiked (^{233}U and ^{244}Pu), and they went through the elemental separation using Dowex anion exchange resin. Later this was replaced with UTEVA ion chromatography resin, because the higher decontamination factor was achieved, i.e. the fractions were cleaner from the other elements. Pu and U were measured by multi-collection TIMS using total evaporation method. The ages (Table 6) were calculated from the parent/daughter ratios using the equations obtained from the Fig.10.

Table 6. Determined ages in years $\pm 2\sigma$ by ID-TIMS (January 2000).

Sample	$^{238}Pu/^{234}U$	$^{239}Pu/^{235}U$	$^{240}Pu/^{236}U$	Δ^1	Δ^2	Δ^3
SRM 946	28.2 ± 0.3	28.6 ± 0.3	28.6 ± 0.3	-3.0	-1.5	-3.9
SRM 947	28.0 ± 0.8	28.2 ± 0.2	28.2 ± 0.2	-1.8	-3.0	-3.8
R1	31.7 ± 0.2	32.1 ± 0.2	31.8 ± 0.2	-1.5	0.9	-
R2	24.5 ± 3.4	31.3 ± 0.2	30.7 ± 0.2	-4.5	-5.5	-

Δ^1 = difference (in %) of the age from the $^{240}Pu/^{236}U$ ratio to the determined age from the $^{241}Pu/^{241}Am$ ratio by gamma-spectrometry.

Δ^2 = difference (in %) of the age from the $^{240}Pu/^{236}U$ ratio to the reported age (data obtained from the NBL files for the SRM 946 and 947, or from the package notes for the R1 and R2).

Δ^3 = difference (in %) of the age from the $^{240}Pu/^{236}U$ ratio to the age determined by alpha-spectrometry in [75].

The ages from different Pu/U ratios of SRM samples agree well with each other. This shows that during the preparation of the material (i.e. reprocessing), the U has been separated effectively from Pu. In the case of samples R1 and R2, small excess of U can been recognised, thus ages differ slightly. The bigger difference in the age from the $^{238}Pu/^{234}U$ ratio of R2 specimen is explained due to the small abundance of ^{238}Pu (0.007 %), which causes inaccuracy in the measurements. When comparing determined ages between different Pu/U and $^{241}Pu/^{241}Am$ ratios (Table 6, Δ^1), the ages show to have slight disagreement. The explanation for this can be found from two reasons:

1) Traces of ^{241}Am after reprocessing. All the ages from the $^{241}Pu/^{241}$ ratio are slightly higher than from Pu/U ratios, thus Pu/Am separation when preparing the materials, could have been incomplete.
2) Incorrect half-live of ^{241}Pu. Different half-live values for the ^{241}Pu are found in the literature even nowadays (14.29 a [76], 14.35 a [23] and 14.41 a [74]).

As the difference of the lowest and highest value of the half-live of ^{241}Pu in the literature is less than 1 %, and the differences between determined ages from the Pu/U and Pu/Am ratios are 1.5-4.5 % (Table 6), the preferred reason is the Am leftovers from reprocessing. Findings of the ^{243}Am traces by gamma-spectrometry support also this theory.

The results of the SRM 946 and 947 samples were compared also to the data of the preparation of these samples obtained from the old files of NBL, USA (Table 6, Δ^2). No exact dates, when the materials had been prepared, were available due to the old age of the materials.

For the samples R1 and R2, the preliminary estimate of the age was obtained from the package notes of the samples, where the year was indicated. Additionally, a publication was found, where the ages of SRM standards were determined by alpha-spectrometry from the in-grown ^{241}Am, and the comparison between the results was done (Table 6, Δ^3).

6.1.2 Secondary Ion Mass Spectrometry (SIMS)

It is known that the quantitative analysis by SIMS is a rather difficult task due to the different secondary ion yields of the elements. The secondary ion yields vary from matrix to matrix and they also depend on the measurement conditions and the instrument itself. As a result, relative sensitivity factors (RSFs) are applied to correct the differences. In this study, the SRM 946, SRM 947, R1 and R2 samples were used as standards to determine the RSF for the Pu/U ratio, because their ages were known from the earlier bulk analyses by TIMS. As the analysed Pu compounds were different (oxide and sulphate), the RSF was determined for the both matrices (Table 7).

Table 7. Relative sensitivity factors (RSF $\pm 1\sigma$) of different Pu/U ratios by SIMS.

Sample	^{238}Pu/^{234}U	^{239}Pu/^{235}U	^{240}Pu/^{236}U
SRM 946	2.38 ± 0.08	2.36 ± 0.06	2.38 ± 0.06
SRM 947	2.33 ± 0.02	2.25 ± 0.04	2.34 ± 0.03
R1	2.41 ± 0.04	2.36 ± 0.04	2.40 ± 0.02
R2	n.d.	2.40 ± 0.01	2.49 ± 0.09

n.d. = not determined

The average RSF value for $PuSO_4$ samples (i.e. SRM 946 and SRM 947) is 2.34 ± 0.05 and for Pu-oxide (i.e. R1 and R2) 2.41 ± 0.05. The means do not differ significantly because they overlap with their uncertainties. Thus no real differences could be seen. The RSF value of 2.41 was used later in the PuO_2 sample analysis.

When the RFS's for Pu- and U-oxides were determined, no uniform results were obtained (Table 8). This is most probably due to the carbon, which was used as a planchet material and also for coating the particles. Carbon seemed to form clusters, which caused mass interferences (e.g. $^{239}Pu^{12}C$ and $^{235}U^{16}O$) hindering the PuO/UO- and PuO_2/UO_2- analyses (Fig. 11).

Table 8. Relative sensitivity factors for Pu/U-oxide ratios by SIMS.

$^{238}PuO/^{234}UO$	$^{239}PuO/^{235}UO$	$^{240}PuO/^{236}UO$
1.30	0.11	0.30
$^{238}PuO_2/^{234}UO_2$	$^{239}PuO_2/^{235}UO_2$	$^{240}PuO_2/^{236}UO_2$
0.20	0.044	0.076

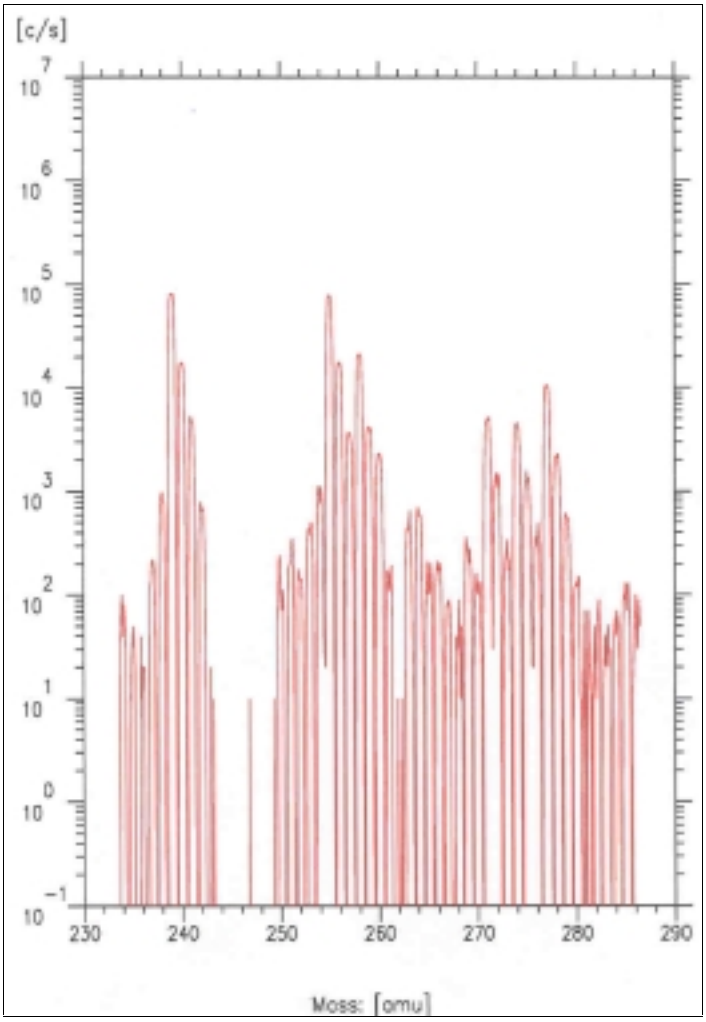

Fig.11. Mass scan of the R1 sample by SIMS.

After the RSF determination, two real samples were analysed. The first one, referred as RR, is a PuO_2 sample from the Round Robin inter-laboratory exercise organised by ITWG [17]. The sample was interesting, because first of its low age (~2 years), which was good to test the limits of the method, and secondly because of the routinely used dating method, gamma spectrometry, did give a remarkably higher age. The reason for this was that some of the Am was co-precipitated with Pu, when the material was precipitated as oxalate. The results for two particles are seen in Table 9. They agree well with the reported age, except the age from the $^{239}Pu/^{235}U$ ratio of the first particle, which gave slightly higher result. This particle had possibly

surface contamination of U or it was interfered by an other kind of particle, because the powder was found to be actually a mixture of four types of particles (Fig.12) [77].

Table 9. Results of particle age determination by SIMS (age in years ±2σ) in February 2000.

RR = Round-Robin test sample (two particles I and II).

F19 = Fund-19 sample (two different PuO_2 particle types 1 and 2).

Sample	Reported age	$^{238}Pu/^{234}U$	$^{239}Pu/^{235}U$	$^{240}Pu/^{236}U$
RR-I	2.3	2.31 ± 0.17	4.77 ± 0.44	2.47 ± 0.02
RR-II		2.35 ± 0.10	2.66 ± 0.26	2.29 ± 0.05
F19-1	20.6	n.d.	*66.2 ± 29.1*	21.5 ± 0.6
F19-2		*1.18 ± 0.07*	*51.9 ± 3.8*	19.9 ± 0.3

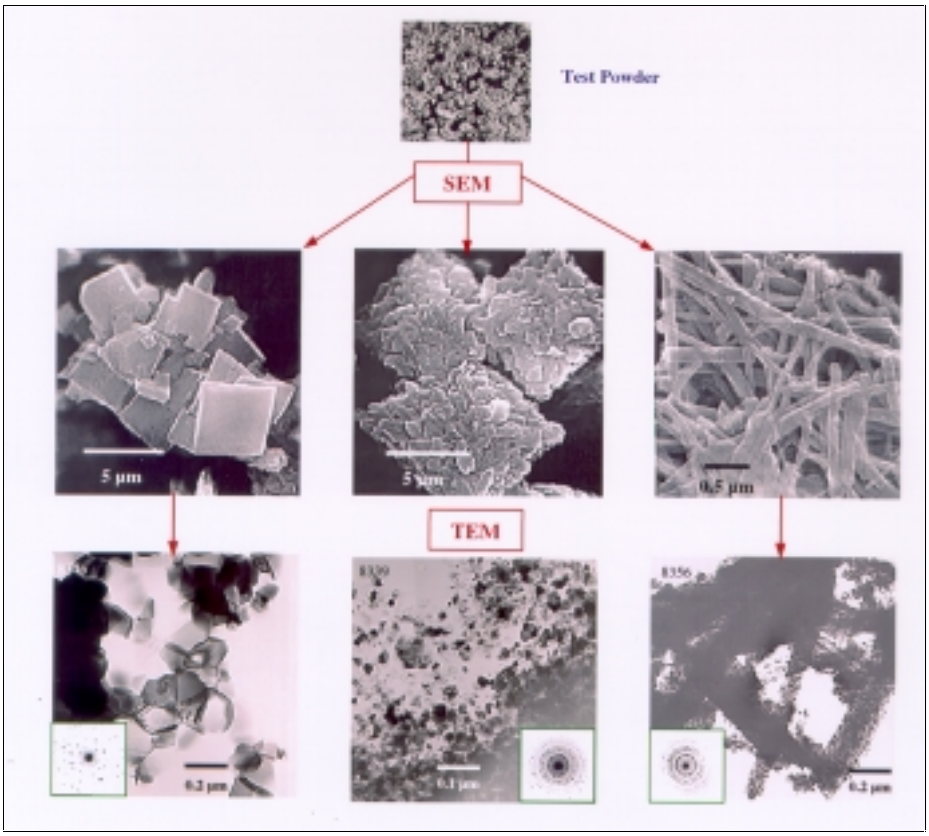

Fig.12. SEM/TEM picture of three types of RR particles [77].

The second analysed sample was Fund-19 (referred here as F19). The F19 is a mixed oxide (MOX) sample, seized at the Munich airport 1994. The age of the sample was determined before for the bulk sample and the result, 20.6 a, was obtained [78]. As being MOX sample, the U particles were interfering in SIMS analyses to the age from the $^{238}Pu/^{234}U$ ratio, where ^{238}Pu has isobaric interference with ^{238}U causing too low age, and age from the $^{239}Pu/^{235}U$ ratio, where the excess of ^{235}U causes too high age (Table 9 in italics). The sample had interesting features, not

only being mixed oxide, but also being mixture of two kinds of PuO_2 particle (Fig.13). This raised a question about the ages of different particle, in other words, have the powders been reprocessed at different times. As the ages of the $^{240}Pu/^{236}U$ ratios show, no remarkable difference could been seen, especially when F19-1 particles being smaller ones, suffer more from the presence of U and thus giving slightly higher age compared to the bigger particles of F19-2.

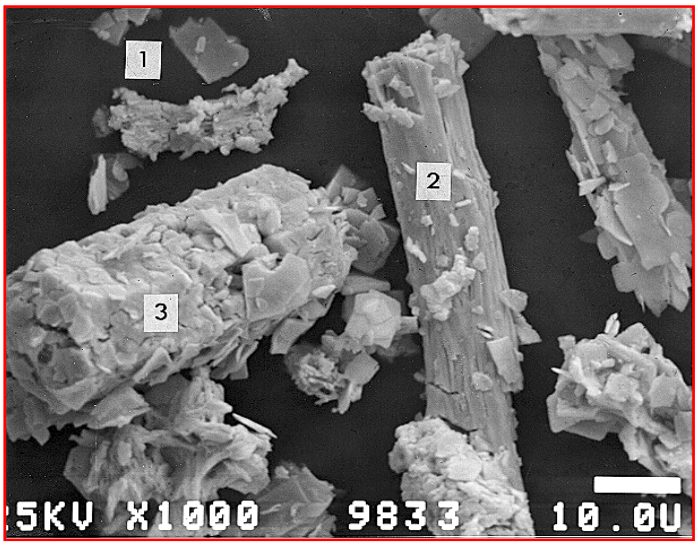

(1) platelets of PuO_2
(2) fibrous rods of PuO_2
(3) rods of U_3O_8

Fig.13. SEM picture of F19 particles [II].

Correcting the U particles contribution to the Pu particles was tried by measuring the Pu isotopic composition of the particles and subtracting the seen ^{238}U surplus in ^{238}Pu, because the Pu isotopic composition was known from the TIMS analysis. The subtraction was performed also to the ^{235}U and ^{236}U isotopes using the isotope ratios of U_3O_8 particles, i.e. $^{235}U/^{238}U = 0.01669$ (± 0.84 %), $^{236}U/^{238}U = 0.000494$ (± 1.4 %). The obtained ages from the $^{239}Pu/^{235}U$ ratios for both Pu particle types showed to be now very low, indicating the possible existence of other source of U contamination. As the Pu particles can contain U leftovers also from the reprocessing, which U composition is unknown, no further correction calculations were attempted.

6.1.3 Inductively Coupled Plasma Mass Spectrometry (ICP-MS)

The ages of SRM 946, SRM 947, R1 and R2 samples were determined also by inductively coupled plasma mass spectrometry to evaluate the capability of the technique in the age determination, which is normally used for trace analysis. The Pu isotopes (mass numbers 238-242) and U isotopes (234-236) were measured using Elan 5000 ICP-MS from Perkin-Elmer [79].

Because of the earlier analyses by TIMS and SIMS, the samples were known to be rather clean from the "external" U and thus no ion chromatography separation was used to separate the ^{238}U from the ^{238}Pu.

Table 10. Determined ages in years $\pm 1\sigma$ by ICP-MS (June 2000).

Sample	**Reported age***	**^{238}Pu/^{234}U**	**^{239}Pu/^{235}U**	**^{240}Pu/^{236}U**	Δ
SRM 946	29.0	22.5 ± 4.1	32.5 ± 6.7	27.3 ± 4.6	-5.9
SRM 947	28.6	25.6 ± 4.5	32.5 ± 6.6	33.9 ± 6.4	18.5
R1	32.2	30.1 ± 3.1	31.6 ± 4.8	32.6 ± 5.5	1.2
R2	31.1	4.0 ± 1.7	35.7 ± 4.0	32.2 ± 9.5	3.5

** = by ID-TIMS in [I].*

Δ = the difference of the age (in %) from the ^{240}Pu/^{236}U ratio to the reported age.

The concentrations of the analysed sample solutions were adjusted to ~100 ppb. This resulted ≤ 5 $\times 10^5$ counts per second (cps) for the highest isotope, ^{239}Pu, but only 2-5 $\times 10^2$ cps for the U isotopes. As the average count rate of the U isotopes in blank was ~ 5 $\times 10^1$ cps, the precision of the U isotope measurements was poor. The standard deviations for 30 replicates/sample varied between 10 and 20 %, being in the case of R2 specimen even higher (Table 10). The accuracy for the R1 and R2 samples was reasonable good from the ^{240}Pu/^{236}U ratio, but for the SRM 946 and especially for the SRM 947 too low. The exact explanation for this is unknown, even if the count rate of the SRM 947 was about two times lower than for other samples. An explanation can be in the sample matrix of the SRM standards, which is sulphate, which can possibly cause some difficulties in the ICP-MS even if very diluted samples were in question.

The results are not corrected for the mass discrimination. It is known that in the ICP-MS heavier isotopes are preferred. This would cause too low ages. Because the precision of the analyses was so low, the effect of the mass discrimination was considered to be negligible.

6.2 Reactor type determination

The isotopic correlation technique was applied to determine the reactor type, where the Pu material is originating from. The isotopic compositions of Pu in spent fuels of most common commercial (LWR, graphite- and gas-moderated-LWR, CANDU, fast reactor) and research reactors (36 % and 90 % ^{235}U enriched MTR and 90% ^{235}U enriched Triga) were calculated by

ORIGEN2 and SCALE computer codes. The determined isotopic compositions of the six samples were then compared to the calculated Pu compositions.

In the absence of the information from fission products and uranium isotopes, only the correlations between Pu-isotopes themselves could be used. As it is traceable to neutron capture and fission cross sections of different Pu-isotopes, the best correlation to illustrate the differences between the reactor types is the correlation given in Fig.14. There the ^{238}Pu abundance reflects the information about the initial ^{235}U enrichment, because the ^{238}Pu is mainly produced through the neutron captures from the ^{235}U and the ^{242}Pu/^{240}Pu ratio indicates hardness of the neutron spectrum (i.e. the harder spectrum the less heavier Pu-isotopes are produced via neutron capture). In addition to the reactor type deduction figure in [III], here in Fig.14 the Magnox reactor type curve and the F19 sample are included. This is to replenish the group of the commercial reactor types, even if Magnox is used only in few countries. The F19 sample case was, on the other hand, still open in the Euratom Safeguards Directorate, when the reactor type deduction was performed to the other samples, thus it was then left out.

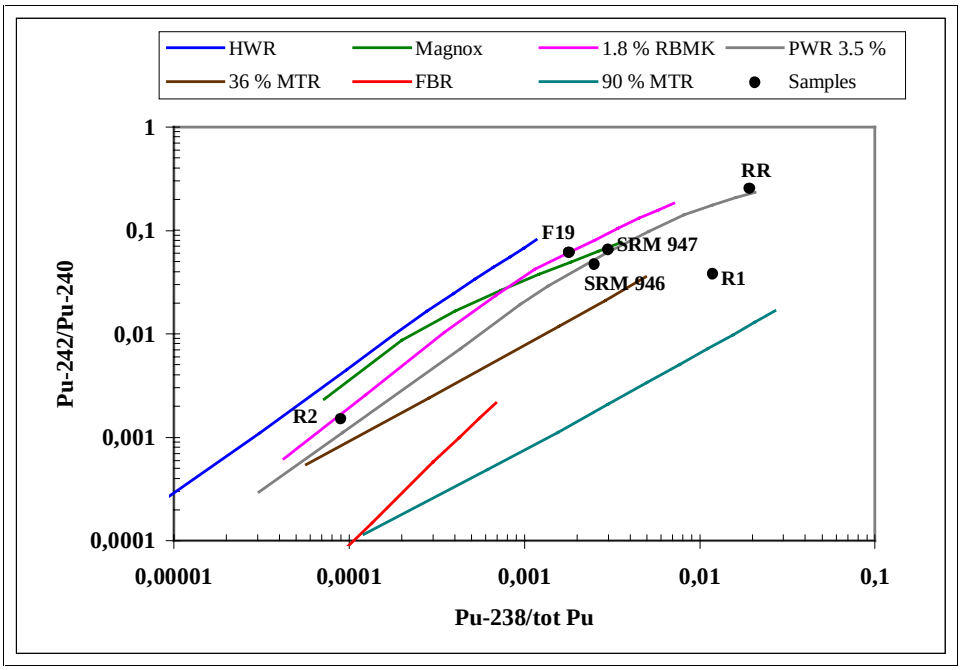

Fig.14. A correlation to deduce the reactor type of Pu samples.

In LWRs and RBMKs, many initial ^{235}U enrichments are used. Thus in Fig.14, only the ends of the typical enrichments were drawn (i.e. 1.8 % RBMK and 3.5 % LWR), when all the rest place between them. Due to the similar neutron spectra, it is impossible to separate PWR and BWR from each other. The RBMK is, however, possible to separate from the rest LWRs using

correlation presented in Fig.15. This is due to the softer spectrum in RBMKs, which produces more ^{240}Pu than in the other LWRs.

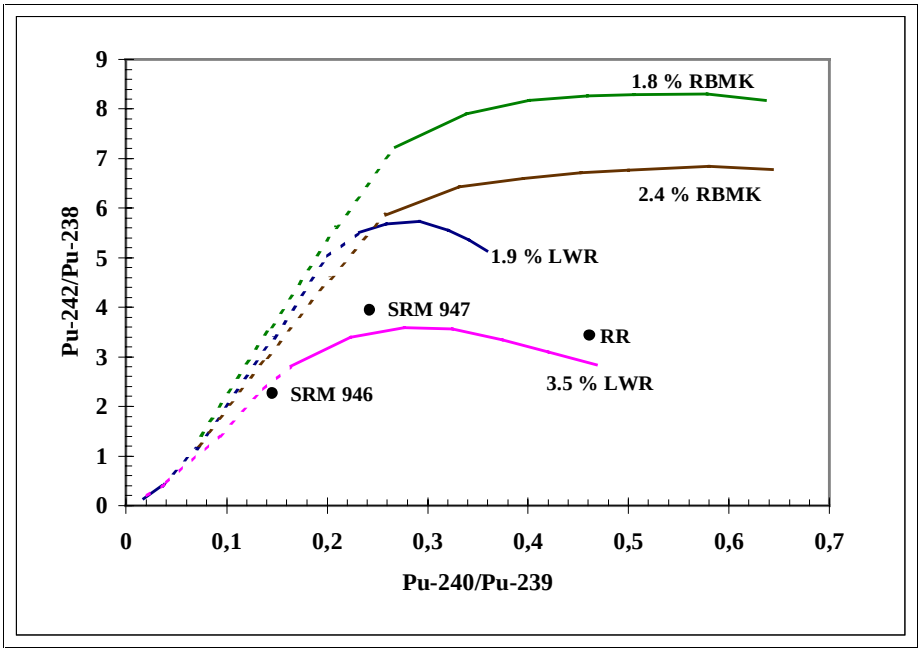

Fig.15. A correlation to distinguish between LWR and RBMK reactor Pu.

In geology and cosmochemistry, where the isotopic correlation technique is used regularly to distinguish the isotopic anomalies, it is recommended to use three-dimensional plots with the same reference isotope. This would, in the case of seven different reactor types, make rather complicated and tangled plots. Thus here, another kind of approach was used. The three isotope ratios, ^{238}Pu/^{240}Pu, ^{239}Pu/^{240}Pu and ^{242}Pu/^{240}Pu, of the sample were compared to the calculated isotope ratios of the reactor types, which were nearest to the sample in Fig.14. This is demonstrated for the samples SRM 947, RR and F19 in Fig.16-18.

In the Figures 16-18, the possible reactor and fuel types are given with their initial ^{235}U enrichment and final burn-up (in parenthesis). The differences between the isotope ratios of the sample and calculations are presented in bars, but also the exact values are given in the tables below. For the sample RR, the best fits are found with the BWR 3.5 % ^{235}U (35 GWd/tHM), PWR 3.1 % ^{235}U (35 GWd/tHM) and PWR 3.5 % ^{235}U (40 GWd/tHM). For the SRM 947, the Magnox reactor, which in Fig.14 could be a possible origin, can be excluded on the grounds of the Fig.17. The best fits are obtained for the BWR 3.0 % ^{235}U (12 GWd/tHM) and PWR 3.5 % ^{235}U (15 GWd/tHM). The F19, which in Fig.14 places on the curve of 1.8 % ^{235}U enriched RBMK, shows in Fig.18 that it does not originate from any commercial reactor type.

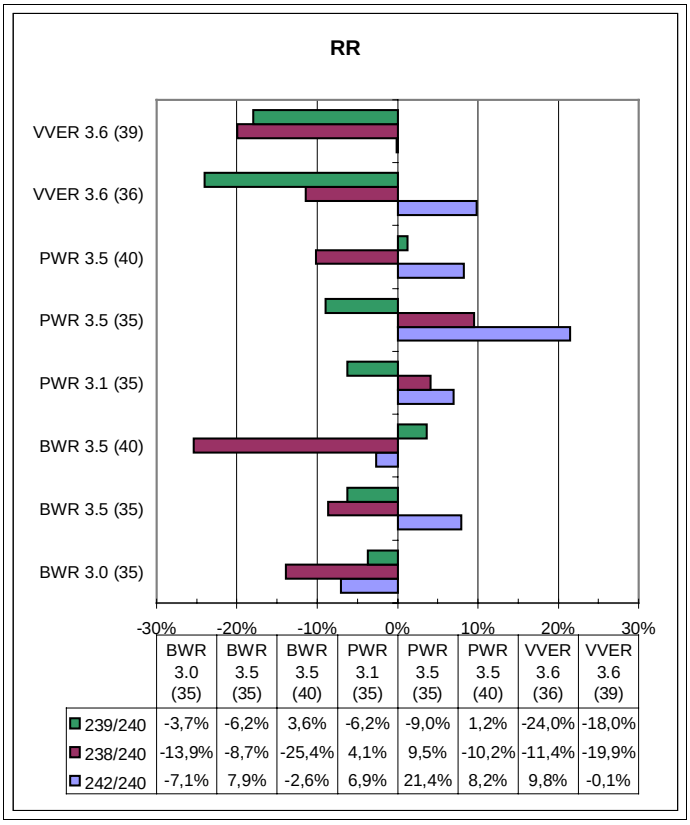

	BWR 3.0 (35)	BWR 3.5 (35)	BWR 3.5 (40)	PWR 3.1 (35)	PWR 3.5 (35)	PWR 3.5 (40)	VVER 3.6 (36)	VVER 3.6 (39)
239/240	-3,7%	-6,2%	3,6%	-6,2%	-9,0%	1,2%	-24,0%	-18,0%
238/240	-13,9%	-8,7%	-25,4%	4,1%	9,5%	-10,2%	-11,4%	-19,9%
242/240	-7,1%	7,9%	-2,6%	6,9%	21,4%	8,2%	9,8%	-0,1%

Fig.16. The Pu isotope ratios of RR compared to possible reactor and fuel types.

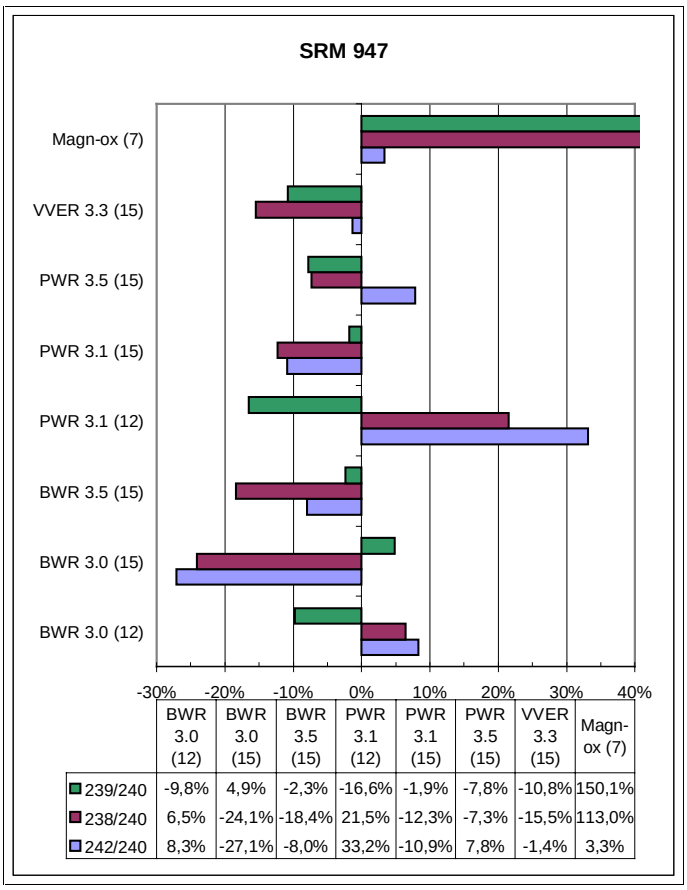

	BWR 3.0 (12)	BWR 3.0 (15)	BWR 3.5 (15)	PWR 3.1 (12)	PWR 3.1 (15)	PWR 3.5 (15)	VVER 3.3 (15)	Magn-ox (7)
239/240	-9,8%	4,9%	-2,3%	-16,6%	-1,9%	-7,8%	-10,8%	150,1%
238/240	6,5%	-24,1%	-18,4%	21,5%	-12,3%	-7,3%	-15,5%	113,0%
242/240	8,3%	-27,1%	-8,0%	33,2%	-10,9%	7,8%	-1,4%	3,3%

Fig.17. The Pu isotope ratios of SRM 947 compared to possible reactor and fuel types.

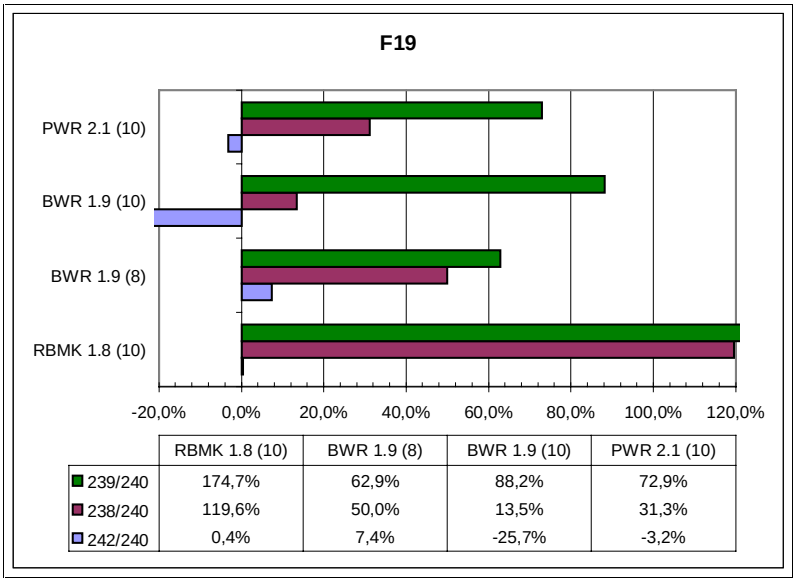

	RBMK 1.8 (10)	BWR 1.9 (8)	BWR 1.9 (10)	PWR 2.1 (10)
239/240	174,7%	62,9%	88,2%	72,9%
238/240	119,6%	50,0%	13,5%	31,3%
242/240	0,4%	7,4%	-25,7%	-3,2%

Fig.18. The Pu isotope ratios of F19 compared to possible reactor and fuel types.

The obtained results from the Fig.14-18 are summarised in Table 11. Even in the cases of R1 and F19, where the reactor type was not found, all commercial reactor types could be excluded. In the case of R1, which was suspected to be a mixture of two fuels, the calculated 60%/40% mixture of VVER 3.6 % ^{235}U (15 GWd/tHM) fuel and MTR 90 % ^{235}U (300 GWd/tHM) spent fuel was found to be rather near the sample composition. Some efforts were also made to determine to the burn-up and initial enrichment, but this with less success. This is understandable considering this simple approach of the isotopic correlation. Additionally one has to recall that:

1. In the ORIGEN2 calculations, the irradiation was assumed to be continuous and no cooling time correction was made.
2. The calculations have rather large error bars, especially for less abundant Pu isotopes in BWR (see Chapter 4.1.3.).
3. The nuclear engineering handbook, where most of the information was obtained, is not complete and some data (i.e. different enrichments in the same reactor) is missing.
4. Often many batches are reprocessed at the same time and thus the recovered Pu can be a mixture of a few spent fuel batches.

Table 11. Summary of the reactor type determination.

Sample	Known data	Information from the isotopic correlation graphs			Information obtained from producer etc.
		Reactor type	^{235}U enrichment	Burn-up (GWd/tHM)	
SRM 946	Isotope standard from USA	LWR	> 3.5 %	~ 15	PWR, Yankee, 3.7 %, 11.3 GWd/tHM
SRM 947	Isotope standard from USA	LWR	~ 3 %	~ 10	BWR, Dresden 1, 1.5-2.5 %, 24.2 GWd/tHM
R1	Originates from Russia	None of the commercial or known research reactors; mixture ?	-	-	-
R2	Originates from Russia	Graphite-moderated-LWR	~ 2 %	1-2	-
RR	European fuel	LWR	3.0-3.5 %	35-40	PWR, 3.28 %, 34-36 GWd/tHM
F19	-	None of the commercial or known research reactors	-	-	-

Even if the reactor type is one of the key parameters in the origin determination, it is not alone enough to reveal the reprocessing plant, where the spent fuel was reprocessed. In addition chemical and material properties (e.g. impurities, platelet and grain sizes) play important role because they tell about the used process itself, which normally varies depending on the fabrication plant. However, a databank is needed to interpret this kind of data. In this study these parameters were beyond the aim.

6.3 Multi-Micro-Channeltron Thermal Ionisation Mass Spectrometer

The detector configuration of the Multi-Micro-Channeltron Mass Spectrometer (MMC-TIMS) was slightly modified since it had been presented in [IV]. The L1 Channeltron (i.e. the first Channeltron on the low mass side from the axial Faraday/Daly detector) was replaced by a Faraday cup, because there was no need for four Channeltrons in the array. Thus now for the ion counting, four detectors (Channeltrons L4-L2 and the Daly) are used, which is enough to measure the most important U isotopes, i.e. ^{234}U, ^{235}U, ^{236}U and ^{238}U. For the age determination only three isotopes, ^{234}U, ^{235}U and ^{236}U, are of interest and the Daly detector can be left out. Pu cannot be measured by the MMC-TIMS, because the ion source is not attached to a glove-box, and thus the contamination risk is high.

The first task was to check the stability of the Channeltrons. It is known that Channeltrons suffer from the ageing effect, i.e. they loose their efficiency with time [50]. Two sets of

measurements were performed with a time lapse of six months, each set lasting around a week (Table 12). The ageing effect is seen to be small over a few days, but discernible for the L2 and L3 Channeltrons being 6-12 % in the first and ~ 4 % in the second test period. The L4 had problems in the second test period and later it "died" completely. The problem was solved by adjusting the electronical set-ups and the efficiency of the L4 was brought back to the level of the other Channeltrons. As Channeltrons have a kind of "continuous amplification", i.e. they have a curved channel where the electrons are multiplied and not certain number of dynodes, the amplification is dependent on the spot on the entrance area, where the ion hits. This influence can be perceived from the gain values, which sometimes jump randomly. However, even without absolute monotonous trend, the ageing effect can be recognised. Due to this fact, the gain calibration should be repeated every day before sample measurements.

Table.12. Short and long term stability of the Channeltrons gain calibration ($\pm 1\sigma$).

Date	Daly/L2	Daly/L3	Daly/L4
02.03. am	0.00975	0.01232	0.01224
02.03. pm	0.00978	0.01241	0.01241
03.03. am	0.00992	0.01298	0.01265
04.03. am	0.01025	0.01328	0.01306
04.03. pm	0.01010	0.01344	0.01310
05.03. am	0.01022	0.01368	0.01344
08.03. am	0.01011	0.01380	0.01341
09.03. am	0.01037	0.01387	0.01392
10.03. am	0.00959	0.01301	0.01299
10.03. pm	0.00951	0.01313	0.01293
Average	0.00996 (± 3.0 %)	0.01319 (± 4.1 %)	0.01302 (± 3.9 %)
28.09. am	0.01017	0.01392	0.01699
28.09. pm	0.01018	0.01363	0.01735
29.09. am	0.01034	0.01385	0.01912
29.09. am	0.01037	0.01376	0.01935
29.09. pm	0.01050	0.01382	0.01973
30.09. am	0.01039	0.01383	0.02030
30.09. pm	0.01051	0.01411	0.02100
01.10. am	0.01056	0.01426	0.02156
Average	0.01038 (± 1.4 %)	0.01390 (± 1.4 %)	0.01943 (± 8.3 %)

Next, the performance of Channeltrons was tested by measuring uranium U-500 standard in the double filament system and using the total evaporation method. The certified values of the $^{234}U/^{238}U$, $^{235}U/^{238}U$ and $^{236}U/^{238}U$ ratios of the U-500 standard are 0.010422, 0.999698 and 0.001519, respectively. Three sample sizes (100, 50 and 10 pg) were used. The 50 pg sample amount gave a sufficiently high signal of 3 mV ≅ 180 000 counts per second (cps) on the ^{235}U and ^{238}U for few minutes. The results in Table 13 shows that for the $^{235}U/^{238}U$ ratio reasonable accuracy and precision was obtained regardless of the sample size. The $^{234}U/^{238}U$ and $^{236}U/^{238}U$

ratios, however, suffered from the high background, which was noticed existing in all half masses (Fig.19). The background is not constant, varying from a few hundred of cps to thousands of cps (Table 13). Thus, the minor isotope measurements of the U-500 sample, where the count rates of ^{234}U and ^{236}U are only ~1900 and 270 cps are to be expected, could not be performed. Until now, the instrument manufacturer could not solve this problem.

Table 13. Results of the U-500 standard by MMC-TIMS (±1σ).

Sample amount	$^{234}U/^{238}U$	$^{235}U/^{238}U$	$^{236}U/^{238}U$	^{235}U total current (V)	Background cps 234	235	236	238
100 pg	0.0094224	1.0266686	-	0.40	2409	2331	2775	4919
"	0.0079966	1.0305115	-	1.45	641	522	463	575
"	0.0022858	1.0594599	-	1.10	1722	1450	1494	4138
"	0.0041939	0.9929254	-	0.21	1006	756	659	1209
"	0.0078414	0.9953231	-	0.27	547	472	472	903
"	0.0085718	0.9955448	0.0007519	0.20	431	659	309	272
"	-	0.9771249	-	0.18	5309	7822	3681	7778
"	0.0078743	0.9912534	-	0.60	672	547	503	781
Average	**0.0068837 (± 38 %)**	**1.0086015 (± 2.7 %)**	**0.0007519**					
Bias	- 34 %	+ 0.89 %	- 51 %					
50 pg	0.0091227	0.9808046	0.0005903	0.14	666	606	500	650
"	0.0067277	0.9741435	-	0.37	863	681	713	1959
"	0.0030255	1.0348519	-	0.35	1088	775	838	3347
"	0.0018690	1.0033794	-	0.32	972	713	622	1750
"	-	1.0457472	-	0.26	1816	1691	1513	5247
"	0.0085008	1.0405884	0.0000224	0.036	266	316	266	50
"	0.0056571	0.9738184	-	0.059	569	491	434	613
"	0.0088455	0.9728168	0.0001886	0.23	494	469	453	388
Average	**0.0062498 (± 46 %)**	**1.0032688 (± 3.2 %)**	**0.0002671 (± 109 %)**					
Bias	- 40 %	+ 0.36 %	- 82 %					
10 pg	0.0090329	1.0113981	-	0.081	491	447	422	347
"	-	1.0221910	-	0.034	1228	1009	897	2331
"	0.0050572	0.9995712	-	0.081	563	491	478	900
"	-	1.0356489	-	0.030	1716	1188	1134	3278
"	-	0.9963684	-	0.066	2053	1647	1163	2272
"	0.0021651	0.9556537	-	0.018	397	366	331	441
"	-	0.9693979	-	0.027	903	669	638	1116
"	-	1.0011649	-	0.022	928	578	938	463
"	-	0.9693576	-	0.033	1378	953	1256	1088
Average	**0.0054184 (± 64 %)**	**0.9956391 (± 2.7 %)**	-					
Bias	- 48 %	- 0.41 %	-					

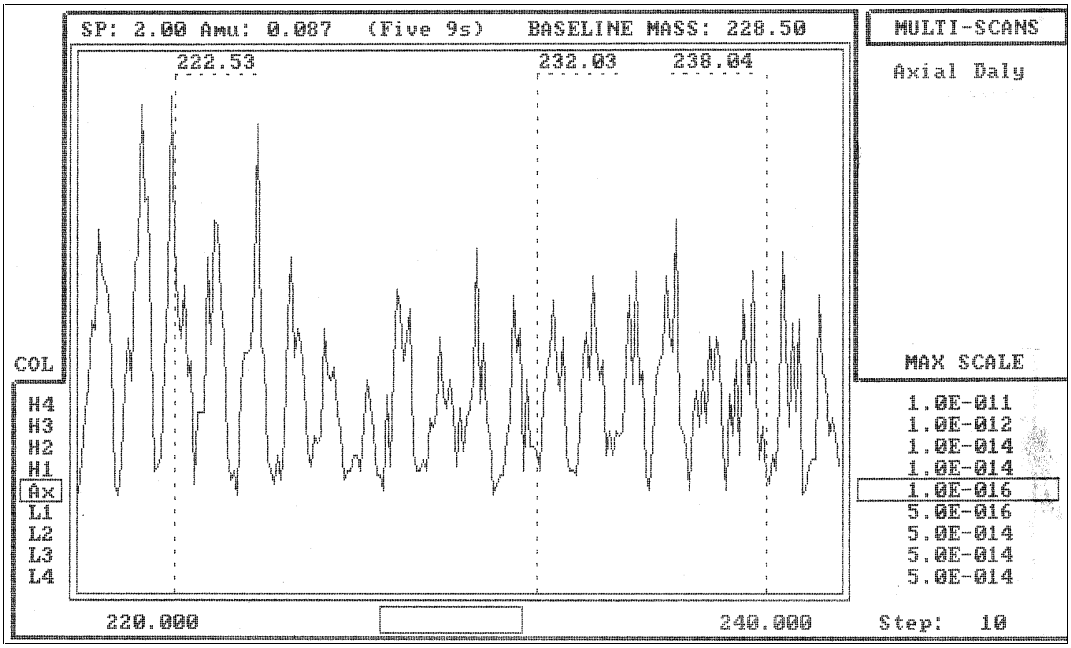

Fig.19. Typical background spectrum scanned from the mass 220 to 240 by MMC-TIMS.

Uranium fractions of the R1 and R2 samples were measured with the MMC-TIMS to compare the results with the multi-collector Faraday cup results obtained in [I]. The results presented in Table 14, show to be much better compared to the earlier U-500 results. This is due to the U ratios, which are near unity in these samples. When going towards lower ratios (e.g. the $^{234}U/^{235}U$ ratio of R2), the effect of the background is seen again, causing large negative bias.

Table 14. Results of the uranium fractions of the R1 and R2 by MMC-TIMS (±1σ).

Sample	$^{234}U/^{235}U$	$^{236}U/^{235}U$
R1-1	3.7168489	0.7303831
R1-2	3.6067998	0.7293618
R1-3	3.6866094	0.7293618
R1-4	3.5881064	0.7140720
R1-5	3.5762641	0.7201290
R1-6	3.5801591	0.7164839
R1-7	3.5925902	0.7247230
R1-8	3.5607755	0.7337143
Average	**3.61352 (± 1.6 %)**	**0.72598 (± 1.2 %)**
[I]	3.63851 (± 0.016 %)	0.73710 (± 0.016 %)
Bias	**- 0.69 %**	**- 1.5 %**
R2-1	0.0174920	0.1690021
R2-2	0.0161506	0.1690330
R2-3	0.0151938	0.1690148
R2-4	0.0154819	0.1716953
R2-5	0.0164257	0.1705017
R2-6	0.0133354	0.1708411
R2-7	0.0137887	0.1737765
Average	**0.01564 (± 17 %)**	**0.17139 (± 2.0 %)**
[I]	0.01674 (± 0.12 %)	0.17598 (± 0.018 %)
Bias	**- 6.6 %**	**- 2.6 %**

In summary, at the moment the MMC-TIMS can be used to measure a few tens pg of U/filament by total evaporation method, which is ~ 1000 times less than with conventional Faraday-TIMS. This is, however, valid only for isotope ratios near unity, i.e. the isotopes, which give signal high enough and thus are not affected by the high background. When the background problem is solved, then even smaller sample sizes can probably be measured because the maximum counting rate can be reduced.

7. Conclusions

Plutonium is a very radiotoxic element, possessing not only a health hazard, but also in a view of non-proliferation of nuclear weapons. The concern of state authorities around Pu intensified in the beginning of 1990's, when smuggling cases of nuclear weapon material were revealed. For the seized Pu material, its origin determination is one of the first and main points to be found out. The age and the reactor type, in which the Pu was produced, are two of the major parameters to be determined in order to unravel the origin.

The age determination of bulk and particle samples can be performed by TIMS and SIMS, respectively. The ages of the bulk samples agree within 1 % for the three different Pu/U ratios, $^{238}Pu/^{234}U$, $^{239}Pu/^{235}U$ and $^{240}Pu/^{236}U$, as determined by IDMS. When compared to the gamma-spectrometric measured age from the $^{241}Pu/^{241}Am$ ratio, which is a routinely used for age determination, small disagreements between the ages were noticed. One explanation could be the Am leftover after reprocessing, the other, with less extent, an incorrect ^{241}Pu half-live. This observation shows the importance of determining the age from two independent, i.e. Pu/U and Pu/Am, parent/daughter relations.

In particle age determination, SIMS proved to be a sensitive analytical tool. However, to obtain accurate results, a special care has to be taken, first in sample preparation, in order not to cross-contaminate it, and secondly in using the appropriate relative sensitivity factor. The attractive feature of particle age determination is the possibility to "look into" mixture of powders. By SIMS different ages of particles in mixtures can be found, which is not the case in bulk sample analysis. Even more important is the possibility to determinate the age of Pu particles released to the environment in a view of the pending Fissile Material Cut-off Treaty. Contrary to enriched ^{235}U production where the present baseline has to be established by numerous analyses, the violation of Pu production could be perceived from the age of its particles.

As a third technique for age determination, the direct injection ICP-MS was tested. An advantage of the ICP-MS is its higher sensitivity compared to conventional TIMS, but on the other hand, it suffers in accuracy. However, for a first indication of the age, ICP-MS has a place due to its simple sample preparation and fast analytical procedure.

The second parameter, i.e. the reactor type, can be determined using the isotope correlation technique. The isotope ratios of the samples were compared to ORIGEN2 and SCALE computer code calculated isotope ratios. The reactor types, where the Pu samples originate from, were found out for most of the cases. For more detailed information, e.g. burn-up

and initial ^{235}U enrichment, the ICT suffered from lack of the accuracy of the simplifying computer codes. As the produced Pu can be a mixture of several reprocessed spent fuel batches, the blending would falsify the original Pu composition anyway.

A new detector type TIMS, Multi-Micro-Channeltron-TIMS was tried in order to reduce the sample sizes required for TIMS analysis. The small size Channeltrons used in array for multi-collection, which has been possible before only for the less sensitive Faraday cups, was demonstrated. Only a few tens of pg of U was needed for total evaporation technique. However, limitations for the low abundant isotopes were met, because of high background found in half masses. The reason for this was not clear and thus the minor isotopes with less than few per cent in content, cannot be determined accurately by this approach.

In summary, the origin determination of Pu could be demonstrated successfully in this study. State authorities are now in a position to find out the possible source of illicit trafficked Pu, and to monitor within the pending fissile material cut-off treaty the production of Pu.

8. References

[1] D.Albright, L.Barbour, Separated inventories of civil plutonium continue to grow, ISIS Plutonium Watch, May 1999

[2] IAEA database on illicit trafficking incidents, open information, 1999-09-01

[3] G.A.Cowan, Sci.Amer., Vol. 235 (1), 1976, 36-47

[4] R.Naudet, Interdisciplinary Science Reviews, Vol. 1 (1), 1976, 72-84

[5] P.M.Grant, K.J.Moody, I.D.Hutcheon, D.L.Phinney, R.E.Whipple, J.S.Haas, A.Alcaraz, J.E.Andrews, G.L.Klunder, R.E.Russo, T.E.Fickies, G.E. Pelkey, B.D.Andresen, D.A.Kruchten, S.Cantlin, Nuclear forensics in law enforcement applications, J.Radioanal. Nucl.Chem. Vol 235, No.1-2, 1998, 129-132

[6] P.M.Grant, K.J.Moody, I.D. Hutcheon, D.L.Phinney, J.S.Haas, A.M.Volpe, J.J.Oldani, R.E.Whipple, N.Stoyer, A.Alcaraz, J.E.Andrews, R.E.Russo, G.L.Klunder, B.D.Andresen, S.Cantlin, Forensic analyses of suspect illicit nuclear material, J.Foren.Sci. 43(3), 1998, 680-688

[7] B.Hileman, Nuclear theft poses growing security threat, C&EN, Sept.11, 1995, 24-25

[8] P.Williams, P.N.Woessner, The real threat of nuclear smuggling, Sci. Amer., Jan 1996, 40-44

[9] A.Schaper, Nuclear smuggling in Europe – real dangers and enigmatic deceptions, presentation at the Forum on Illegal Nuclear Traffic: Risks, Safeguards and Countermeasures, Como, Italy,11-13.6.1997

[10] J.H.Nuckolls, Post-cold war nuclear dangers: Proliferation and terrorism, Science 267, 1995, 1112-1114

[11] IAEA General Conference, GC(42)/17, 1998

[12] IAEA General Conference, GC(40)/15, 1996

[13] S.Thorstensen, Safeguards & illicit nuclear trafficking: Towards more effective control, IAEA Bulletin, 4/1996, 29-31

[14] F.von Hippel, Fissile material security in the post-cold-war world, Phys. Today, June 1995, 26-31

[15] L.Koch, S.Niemeyer, Status of International Co-operation on Nuclear Smuggling Forensic Analysis, March 20, 1996

[16] L.Koch, S.Niemeyer, N.Nikiforov, G.Mason, G.M.J.Herbillon, International cooperation in combating illicit trafficking of nuclear materials by technical means, Proceedings of the 21st Annual ESARDA Symposium, May 1999, 805-810

[17] G.Dudder, G.Herbillon, Plutonium Round Robin Test - Final Report, ITWG, May 2000

[18] G.Herbillon, G.Dudder, Status of HEU Round-Robin exercise, 6th ITWG meeting in Vienna, Austria, June 2000

[19] G.Faure, Principles of isotope geology, 2nd edition, John Wiley & Sons, New York, 1986

[20] Yu.Dolgov, Yu.Bibilashvili, N.Chorokhov, L.Koch, R.Schenkel, A.Schubert, Case studies with a relational database system for identification of nuclear material of unknown origin, Proceedings of the Russian International Conference on Nuclear Material Protection, Control and Accounting, Obninsk, Russia, 9-14 March 1997, 116-120

[21] Yu.Dolgov, Yu.Bibilashvili, N.Chorokhov, A.Schubert, G.Janssen, K.Mayer, L.Koch, Installation of a database for identification of nuclear material of unknown origin at VNIINM Moscow, Proceedings of the 21st Annual ESARDA Symposium, May 1999, 831-838

[22] A.Schubert, G.Janssen, L.Koch, P.Peerani, Yu.K.Bibilashvili, N.A.Chorokhov, Yu.N.Dolgov, A software package for nuclear analysis guidance by a relational database, Proceedings of the ANS International Conference on the Physics of Nuclear Science and Technology, New York, 5-8 October 1998, 1385-1392
[23] G.Pfennig, H.Klewe-Nebenius, W.Seelmann-Eggeberg, Chart of Nuclides, 6th edition, 1995
[24] K.H.Lieser, Nuclear and Radiochemistry: Fundamentals and Applications, 1997
[25] O.J.Wick (editor), Plutonium Handbook, A Guide to the Technology - Volumes I & II, 1980
[26] G.Choppin, J.Rydberg, J.O.Liljentzin, Radiochemistry and Nuclear Chemistry, 2nd Edition, 1995
[27] J.Lamarsh, Introduction to Nuclear Engineering, 2nd Edition, Addison-Wesley, 1983
[28] S.Fetter, F.von Hippel, A step-by-step approach to a fissile cutoff, Arms Control Today, Vol. 25, No. 8, 1995, 3-8
[29] R.Berg, C.Foggi, L.Koch, R.Kraemer, F.J.Woodman, Value and use of isotopic correlations in irradiated fuels, Practical Applications of R&D in the Field of Safeguards, Proceedings of the ESARDA Symposium, Rome, Italy, 7-8 March 1974, 183-211
[30] S.Guardini, G.Guzzi, Reference data on post irradiation analysis of light water reactor fuel samples, EUR 7879 EN, 1982
[31] L.Stanchi (editor), Proceedings of the ESARDA Symposium on the Isotopic Correlation and its Application to the Nuclear Fuel Cycle, Stresa, Italy, 9-11 May 1978
[32] M.J.Bell, ORIGEN – The ORNL isotope generation and depletion code, ORNL-4628, Oak Ridge National Laboratory, 1973
[33] U.Fischer, H.W.Wiese, Verbesserte konsistente Berechnung des nuclearen Inventars abgebrannter DWR-Brennstoffe auf der Basis von Zell-Abbrand-Verfahren mit KORIGEN, KfK 3014, January 1983
[34] SCALE 4.4: Modular code system for performing Standardised Computer Analyses for Licensing Evaluation, RSICC-CCC-545, Oak Ridge National Laboratory, 1998
[35] A.G.Croff, ORIGEN2: A versatile computer code for calculating the nuclide composition and characteristics of nuclear materials, Nucl. Technology, Vol. 62, 1983, 335-352
[36] A.G.Croff, A User's Manual for the ORIGEN2 Computer Code, ORNL/TM-7175, Oak Ridge National Laboratory, 1980
[37] P.Peerani, Databank for the identification of unknown nuclear materials: Calculation of spent nuclear fuel composition, ITU internal report, 1997
[38] M.D.DeHart, O.W.Hermann, C.V.Parks, Validation of SCALE depletion method for PWR spent-fuel isotopic characterization, Transactions of ANS, Vol.73, 1995, 361-363
[39] S.K.Aggarwal, H.C.Jain (editors), Introduction to Mass Spectrometry, Indian Society for Mass Spectrometry (ISMAS), 1997
[40] I.T.Plazner, Chemical Analysis Vol.145, Modern Isotope Ratio Mass Spectrometry, John Wiley & Sons, 1997
[41] D.Poupard, A.Juery, Isotope fractionation of plutonium in thermal ionization mass spectrometry. Direct deposition and resin bead, Radiochim. Acta 57, 1992, 21-24
[42] J.D.Fassett, W.R.Kelly, Interlaboratory isotopic ratio measurement of nanogram quantities of uranium and plutonium on resin beads by thermal ionization mass spectrometry, Anal. Chem. 56, 1984, 550-556
[43] J.M.Kelley, D.M. Robertson, Plutonium ion emission from carburized rhenium mass spectrometer filaments, Anal.Chem. 57, 1985, 124-130
[44] D.J.Rokop, R.E.Perrin, G.W.Knobeloch, V.M.Armijo, W.R.Shields, Thermal ionization mass spectrometry of uranium with electrodeposition as a loading technique, Anal.Chem. 54, 1982, 957-960
[45] D.H.Smith, J.A.Carter, A simple method to enhance thermal emission of metal ions, Int. J. Mass Spectrom. Ion Phys. 40, 1981, 211-215

[46] M.H.Kakazu, N.M.P.Moraes, S.S.Iyer, C.Rodrigues, Reduction of oxide ions of uranium in single-filament surface-ionisation mass spectrometry with application to rock samples, Anal. Chim. Acta 132, 1981, 209-213

[47] R.E.Perrin, G.W.Knobeloch, V.M.Armijo, D.W.Efurd, Isotopic analysis of nanogram quantities of plutonium by using a SID ionisation source, Int. J.Mass Spectrom. Ion Proc. 64, 1985, 17-24

[48] C.Bergey, J.Cesario, S.Deniaud, Improvements of analytical results of thermal ionization mass spectrometry through electrolytic sample deposition, Int. J. Mass Spectrom. Ion Phys. 48, 1983, 393-396

[49] F.A.White, G.M.Woods, Mass Spectrometry: Applications in science and engineering, John Wiley & Sons 1986

[50] S.Richter, U.Ott, F.Begemann, Multiple ion counting in isotope abundance mass spectrometry, Int. J. Mass Spectrom. Ion Processes 136, 1994, 91-100

[51] K.L.Ramakumar, R.Fiedler, Calibration procedures for a multicollector mass spectrometer for cup efficiency, detector amplifier linearity, and isotope fractionation to evaluate the accuracy in the total evaporation method, Int. J. Mass Spectrom. 184, 1999, 109-118

[52] C.Bayne, D.Donohue, R.Fiedler, Multidetector calibration for mass spectrometers, Int. J. Mass Spectrom. Ion Processes 134, 1994, 169-182

[53] P.De Bievre, Accurate isotope ratio mass spectrometry: Some problems and possibilities, Adv. Mass Spectrom. 7A, 1978, 395-447

[54] L.J.Moore, E.F.Heald, J.J.Filliben, An isotopic fractionation model for the multiple filament thermal ion source, Adv. Mass Spectrom. 7A, 1978, 448-474

[55] K.Habfast, Fractionation in the thermal ionisation source, Int. J. Mass Spectrom. Ion Phys. 51, 1983, 165-189

[56] S.K.Aggarwal, A.I.Almaula, P.S.Khodade, A.R.Parab, R.K.Duggal, C.P.Singh, A.S.Rawat, G.Chourasiya, S.A.Chitambar, H.C.Jain, Determination of K-factors for isotope abundance measurements of uranium and plutonium by thermal ionisation mass spectrometry, J. Radioanal. Nucl. Chem., Letters 87 (3), 1984, 169-178

[57] H.Kanno, Isotope fractionation in a thermal ion source, Bull. Chem. Soc. Jpn 44, 1971, 1808-1812

[58] L.A.Dietz, C.F.Pachucki, G.A.Land, Internal standard technique for precise isotopic abundance measurements in thermal ionization mass spectrometry, Anal. Chem. 34, 1962, 709-710

[59] D.H.Smith, R.L.Walker, Internal standards applied to isotopic ratio measurements of uranium and plutonium, Nucl. Mater. Management 13 (2), 1984, 44-48

[60] M.Romkowski, S.Franzini, L.Koch, Mass-spectrometric analysis of sub-nanocurie samples of uranium and plutonium, Proceedings of the 8th Annual ESARDA Symposium, 12-14 May 1987, 111-113

[61] R.Fiedler, D.Donohue, G.Grabmueller, A.Kurosawa, Report on preliminary experience with total evaporation measurements in thermal ionization mass spectrometry, Int. J. Mass Spectrom. Ion Processes 132, 1994, 207-215

[62] E.L.Callis, R.M.Abernathey, High-precision isotopic analyses of uranium and plutonium by total sample volatization and signal integration, Int. J. Mass Spectrom. Ion Processes 103, 1991, 93-105

[63] R.Fiedler, Total evaporation measurements: Experience with multi-collector instruments and a thermal ionization quadrupole mass spectrometer, Int. J. Mass Spectrom. Ion Processes 146/147, 1995, 91-97

[64] H.Kühn, R.Wellum, Optimisation of information from the total evaporation method for thermal ionisation mass-spectrometry, Proceedings of the 17th Annual ESARDA Symposium, 9-11 May 1995, 389-393

[65] K.G.Heumann, Isotope dilution mass spectrometry, Int. J. Mass Spectrom. Ion Processes 118/119, 1992, 575-592
[66] P.De Bièvre, Isotope dilution mass spectrometry: What can it contribute to accuracy in trace analysis ?, Fresenius J. Anal. Chem. 337, 1990, 766-771
[67] A.Benninghoven, Y.Nihei, R.Shimizu, H.W.Werner (eds.), Secondary ion mass spectrometry: SIMS IX, John Wiley & Sons, 1994
[68] A.Benninghoven, B.Hagenhoff, H.W.Werner (eds.), Secondary ion mass spectrometry: SIMS X, John Wiley & Sons, 1997
[69] G.Tamborini, M.Betti, V.Forcina, T.Hiernaut, B.Giovannone, L.Koch, Application of secondary ion mass spectrometry to the identification of single particles of uranium and their isotopic measurement, Spectrochimica Acta B 53, 1998, 1289-1302
[70] G.Tamborini, M.Betti, Characterisation of radioactive particles by SIMS, Microchim.Acta 132, 2000, 411-417
[71] R.G.Wilson, F.A.Stevie, C.W.Magee, Secondary Ion Mass Spectrometry: A practical handbook for depth profiling and bulk impurity analysis, John Wiley & Sons, 1989
[72] A.Benninghoven, F.G.Rüdenauer, H.W.Werner, Chemical Analysis Vol.86, Secondary Ion Mass Spectrometry: Basic concepts, instrumental aspects, applications and trends, John Wiley & Sons, 1987
[73] Cameca IMS 6F User's Guide, 1995
[74] J.Magill, Nuclides 2000, EUR 18737 EN, 1999
[75] H.W.Kirby, W.E.Sheehan, Determination of ^{238}Pu and ^{241}Am in ^{239}Pu by alpha-spectrometry, Nucl. Instrum. Methods Phys. Res. 223, 1984, 356-359
[76] P.De Bievre, A.Verbruggen, A new measurement of the half-live of ^{241}Pu using isotope mass spectrometry, Metrologia 36, 1999, 25-31
[77] Annual report of the Institute for Transuranium Elements, EUR 19054 EN, 1999, 132-134
[78] Fund 19, ITU internal report, 1994 (restricted distribution)
[79] J.I.Garcia Alonso, F.Sena, P.Arbore, M.Betti, L.Koch, Determinations of fission products and actinides in spent nuclear fuels by isotope dilution ion chromatography inductively coupled plasma mass spectrometry, J. Anal. At. Mass Spectrom. 10, 1995, 381-393

LIST OF ABBREVIATIONS

BWR = Boiling Water Reactor

CANDU = Once-through Canada Deuterium Uranium Reactor

DOE = Department of Energy

FBR = Fast Breeder Reactor

FMCT = Fissile Material Cut-off Treaty

FSU = Former Soviet Union

GDMS = Glow Discharge Mass Spectrometry

HEU = High Enriched Uranium

HWR = Heavy Water Reactor

IAEA = International Atomic Energy Agency

ICP-MS = Inductively Coupled Plasma Mass Spectrometry

IDA = Isotope Dilution Analysis

IDMS = Isotope Dilution Mass Spectrometry

ITWG = International Technical Working Group on Nuclear Smuggling

LEU = Low Enriched Uranium

LMFBR = Liquid Metal Fast Breeder Reactor

LWR = Light Water Reactor

MMC = Multi-Micro-Channeltron

ORIGEN = The ORNL Isotope Generation and Depletion Code

ORNL = Oak Ridge National Laboratories

RBMK = High-Power Channel-Type Reactor (abbreviation from Russian)

RSF = Relative Sensitivity Factor

SCALE = Standardised Computer Analyses for Licensing Evaluation

SEM = Secondary Electron Multiplier / Scanning Electron Microscope

SIMS = Secondary Ion Mass Spectrometry

TEM = Transmission Electron Microscopy

TIMS = Thermal Ionisation Mass Spectrometry

TOF = Time-of-Flight

VVER = Pressurised Water-Water Energetic Reactor (abbreviation from Russian)

```
-1
-1
-1
 RDA    ORIGEN2, VERSION 2.1 (8-1-91) SAMPLE PROBLEM #2
 RDA    * SAMPLE #2 IS A SIMPLE IRRADIATION OF PWR FUEL ONLY
 RDA    UPDATED BY:  SCOTT B. LUDWIG, OAK RIDGE NATIONAL LABORATORY
 BAS    ONE METRIC TON OF PWRU FUEL
 RDA    -1 = FRESH U FUEL WITH IMPURITIES (1 MT)
 RDA    WARNING:  VECTORS ARE OFTEN CHANGED WITH RESPECT TO THEIR CONTENT.
 RDA    THESE CHANGES WILL BE NOTED ON RDA CARDS.
 CUT    5 0.0000000001 -1
 LIP    0 0 0
 LIB    0  1 2 3  601  602  603  9   3   0  1   38
 PHO    0  0  0   10
 TIT    INITIAL COMPOSITIONS OF UNIT AMOUNTS OF FUEL AND STRUCT MAT'LS
 RDA    READ FUEL COMPOSITION INCLUDING IMPURITIES (1000 KG)
 INP    -1   1  -1  -1  1  1
 TIT    IRRADIATION OF ONE METRIC TON OF PWRU FUEL
 MOV    -1   1   0   1.0
 HED    1                          CHARGE
 BUP    Time   Power/flux
 IRP     50.0   40.0    1   2   4 2  END OF THIS STEP=  2,000  MWD/MTIHM
 IRP    125.0   40.0    2   3   4 0  END OF THIS STEP=  5,000  MWD/MTIHM
 IRP    200.0   40.0    3   4   4 0  END OF THIS STEP=  8,000  MWD/MTIHM
 IRP    250.0   40.0    4   5   4 0  END OF THIS STEP=10,000  MWD/MTIHM
 IRP    300.0   40.0    5   6   4 0  END OF THIS STEP=12,000  MWD/MTIHM
 IRP    375.0   40.0    6   7   4 0  END OF THIS STEP=15,000  MWD/MTIHM
 IRP    500.0   40.0    7   8   4 0  END OF THIS STEP=20,000  MWD/MTIHM
 IRP    625.0   40.0    8   9   4 0  END OF THIS STEP=25,000  MWD/MTIHM
 IRP    750.0   40.0    9  10   4 0  END OF THIS STEP=30,000  MWD/MTIHM
 IRP    875.0   40.0   10  11   4 0  END OF THIS STEP=35,000  MWD/MTIHM
 IRP   1000.0   40.0   11  12   4 0  END OF THIS STEP=40,000  MWD/MTIHM
 BUP
 OPTL    24*8
 OPTA     4*8   7 8 8   17*8
 OPTF    24*8
 OUT    -12   1    -1   0
 OUT     12   1    -1   0
 MOV     12   1     0   1.0
         Time
 DEC     1.0   1   2   5   4
 DEC     2.0   2   3   5   0
 DEC     3.0   3   4   5   0
 DEC     5.0   4   5   5   0
 DEC     7.0   5   6   5   0
 DEC    10.0   6   7   5   0
 OUT     -6    1    -1   0
 OUT      6    1    -1   0
 END
 2   942380 0.0   922350 35000.  932370 0.0   922380 965000.      FUEL 3.5%
 2   942390 0.       942400 0.      942410 0.     942420 0.        FUEL IMPU
 4   080000 134454. 090000  10.7   110000  15.0   120000   2.0   FUEL IMPU
 4   130000  1190.  140000 1080.   150000  48.0   170000   5.3   FUEL IMPU
 4   200000  2.0    220000  847.0  230000  3.0    240000   23400 FUEL IMPU
 4   250000  2100.  260000 75500.   270000  120.  280000  25600. FUEL IMPU
 4   290000  10.    300000  40.3   420000  50.    470000   0.1   FUEL IMPU
 4   480000  25.0   490000  2.0    500000  4000.  640000   2.5   FUEL IMPU
 4   740000  2.0    820000  1.0    830000  0.4    0        0.0   FUEL IMPU
 0
```

Reactor and fuel type libraries

Specific power irradiation. IRF = flux

Output options for activation products, actinides and fission products

Decay

Initial fuel composition

Flow diagram of the SAS2H sequence

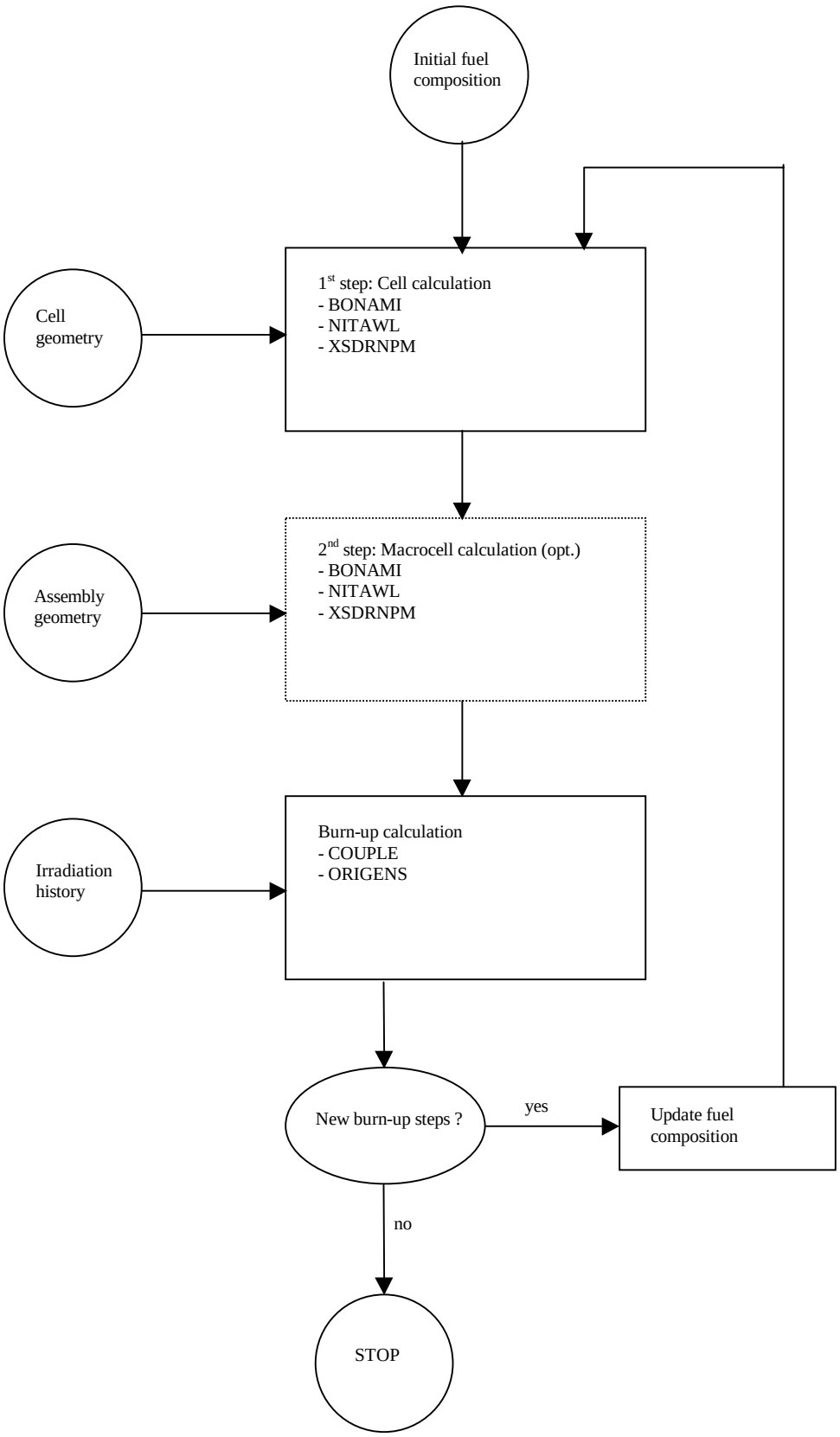

BONAMI: retrieves multigroup cross sections and perform for all the nuclides a preliminary calculation of the self-shielding based on a simplified zero-dimensional method (Bondarenko method)
NITAWL: computes for the main resonant nuclides the self-shielding factors using the Nordheim integral method which takes into account the 1-D pin geometry
XSDRNPM: solves the Boltzmann equation of neutron transport in the 1-D cell geometry, computes the space-energy distribution of neutron flux and average 1-group cross sections
COUPLE: updates ORIGEN libraries with the cross sections and spectral parameters computed by XSDRNPM, creating problem and burnup dependent libraries
ORIGENS: computes the isotopic evolution of fuel composition